



University of Nairobi  
Institute of Nuclear Science and Technology

**DESIGN AND CHARACTERIZATION OF A HYBRID FLAT PLATE  
PHOTOVOLTAIC-THERMAL SYSTEM**

By

NYARIKI ONDARA WYCLIFFE

**A thesis submitted in partial fulfillment of requirements for the degree of  
Master of Science in Nuclear Science in the Institute of Nuclear Science and  
Technology in the University of Nairobi.**

© August 2016

## Declaration

This thesis is my original work and has not been submitted for a degree in any other University.

Signature..... Date.....

Nyariki Ondara Wycliffe (S56/70424/2011)

This thesis has been submitted with the knowledge of the supervisors.

## Supervisors

Mr. David M. Maina  
Institute of Nuclear Science and Technology,  
College of Architecture and Engineering  
University of Nairobi

Signed.....

Date.....

Prof. D. M. Mulati  
College of Pure and Applied Sciences  
Jomo Kenyatta University of Agriculture and Technology

Signed.....

Date.....

## **Dedication**

This thesis is a special dedication to my daughters Yvette and Rita for sharing their joy during my entire research period.

## **Acknowledgements**

I am deeply grateful to my supervisors, Mr David M. Maina and Prof. David M. Mulati for their guidance, insight and encouragement to pursue my research. Their advice, criticism and contribution were invaluable in guiding and inspiring me.

I would also like to thank technologists Mr. Mathias Mailu and Mr. Daniel Njoroge who helped me set-up the experimental rig. Their first-hand experience with the equipment I was using helped me complete my research in record time.

This research would not have been possible without funding from NACOSTI and KNEB. I deeply appreciate the opportunity offered to me to pursue this course.

Finally, I appreciate my parents, brothers, sisters and friends for constantly reminding me of my objectives. My wife Immaculate and daughters Yvette and Rita, thank you for an opportunity to unwind with you during the entire research period as it gave me a renewed spirit to continue day in day out.

## **ABSTRACT**

A variety of solar energy systems have been designed to harness sun power to produce both thermal and electric energy. Hybrid photovoltaic/thermal (PV/T) solar energy harnessing systems can concurrently provide electric and heat energy, thereby ensuring a higher conversion rate of a beam of solar radiation. A well designed PV/T system can minimize temperature influence on the electrical efficiency of a Photovoltaic module by continually cooling it. In this study, simulation results for a model constructed in commercial software TRNSYS for a hybrid PV/T system for low temperature domestic water applications for a typical Kenyan family of five are presented. Further, the results of the prototype PV/T system that was constructed are outlined and discussed. The constructed PV/T system was found to meet over half of the projected water demand. With a payback period of 5.2 years, the PVT system gives a lifetime cost saving of about Kshs. 90, 000. The combined system efficiency averaged 50%. These results are quite promising and they point towards the economic viability of the system for a typical Kenyan household and other applications requiring both electricity and hot water concurrently.

## Table of Contents

Declaration .....	i
Dedication .....	ii
Acknowledgements .....	iii
ABSTRACT .....	iv
List of Figures .....	vii
List of Tables .....	viii
List of Abbreviations .....	ix
CHAPTER 1 .....	- 1 -
INTRODUCTION .....	- 1 -
1.1 Energy today .....	- 1 -
1.2 Solar energy.....	- 1 -
1.2.1 Solar thermal collector.....	- 2 -
1.2.2 Solar Photovoltaic module.....	- 3 -
1.2.3 Photovoltaic-thermal (PV/T) collector .....	- 5 -
1.3 Research Problem.....	- 7 -
1.4 Justification .....	- 7 -
1.5 Scope of the Study.....	- 8 -
1.6 Objectives.....	- 8 -
CHAPTER 2 .....	- 9 -
LITERATURE REVIEW .....	- 9 -
2.1 Introduction .....	- 9 -
2.2 Major Publications on Developments of PV/T Collectors.....	- 9 -
2.3 Photovoltaic-thermal collector characteristics .....	- 12 -
CHAPTER 3 .....	- 15 -
METHODOLOGY .....	- 15 -

3.0 Introduction .....	- 15 -
3.1 Modelling and simulation.....	- 15 -
3.1.1 Determining the demand from the system.....	- 15 -
3.1.2 Modelling Approach.....	- 19 -
3.2 Experimental characterization.....	- 21 -
3.2.1 Layout of the constructed PV/T system .....	- 22 -
3.2.2 Measurements.....	- 24 -
3.2.3 Experimental Procedure .....	- 27 -
CHAPTER 4 .....	- 28 -
RESULTS AND DISCUSSION.....	- 28 -
4.1 Simulation Results and analysis.....	- 28 -
4.1.1 Optimization of the water flow rate.....	- 28 -
4.1.2 Hourly performance of the system .....	- 30 -
4.2 Experimental results and discussion .....	- 32 -
4.2.1 Thermal performance .....	- 32 -
4.2.2 Electrical Performance .....	- 38 -
4.3 Economic Analysis.....	- 39 -
CHAPTER 5: CONCLUSION AND RECOMMENDATIONS .....	- 43 -
5.1 Conclusion.....	- 43 -
5.2 Recommendations .....	- 43 -
References.....	- 44 -
Appendices.....	- 47 -
Appendix A: Experimental Results.....	- 47 -
Appendix A (i): Tables showing results collected from the thermal monitor points .....	- 47 -
Appendix A (ii): Table showing Mini-KLA results collected.....	- 48 -
Appendix B: Kenya solar resource map.....	- 51 -

## List of Figures

Figure 1.1: Figure showing useful and non-useful portions of the sun's photon spectrum.....	- 4 -
Figure 1.2: Schematic diagram of a water cooled PV/T system.....	- 6 -
Figure 3.1: Hot water consumption profile for a family of five .....	- 19 -
Figure 3.2: Information flow diagram for the model constructed in TRNSYS.....	- 20 -
Figure 3.3: Water circulation line behind the PV module .....	- 22 -
Figure 3.4: Schematic view of the experimental PV/T system set-up.....	- 23 -
Figure 3.5: Experimental rig.....	- 24 -
Figure 3.6: Irradiance sensortype Si-01TC-T used to measure solar radiation .....	- 25 -
Figure 3.7: Measuring system for taking I-V curve of the PV module(Mini-KLA) .....	- 26 -
Figure 3.8: Thermocouple attached to a monitor code .....	- 26 -
Figure 4.2: Electrical and thermal energy output from the TRNSYS model within 24 hours	- 30 -
Figure 4.4: The hourly efficiency of the Modelled system on 27 <sup>th</sup> August 2014.....	- 31 -
Figure 4.5: Curve of radiation intensity and average Panel Temperature with water flow. ....	- 33 -
Figure 4.6: Curve of radiation intensity and panel Temperature with no water flow.....	- 33 -
Figure 4.7: Panel temperature profile with and without water flow .....	- 34 -
Figure 4.8: Temperature profile of inlet and outlet water temperatures from the PV/T panel	- 35 -
Figure 4.9: Radiation intensity with variation of temperature gradient at the inlet and outlet	- 35 -
Figure 4.10: Thermal efficiency against time of the day (27 <sup>th</sup> August 2014).....	- 37 -
Figure 4.11: Electrical efficiency against time of the day (27 <sup>th</sup> August 2014).....	- 38 -



## List of Tables

Table 1: Daily load energy demand for a typical Kenyan family of five .....	- 16 -
Table 2: Estimate of hot water required for a five member Kenyan family .....	- 17 -
Table 3: Parameters for the simulation model .....	- 21 -
Table 4: Annual output of electrical and thermal energy for various water flow rates .....	- 29 -
Table 5: Thermal efficiency of the PV/T system (27 <sup>th</sup> August 2014) .....	- 36 -
Table 6: Total amount of heat energy collected(27 <sup>th</sup> August 2014) .....	- 37 -
Table 7: Table showing the PV/T panel efficiencies on 27th August 2014 .....	- 39 -
Table 8: The cost of buying 57.42Kwh of power from KPLC .....	- 40 -
Table 9: Cost of the additional components to modify the PV module to PV/T collector. ....	- 41 -

## List of Abbreviations

PSH: Peak Sun hours

$\rho$ : Density of water

$A_c$ : Function of the collector area ( $m^2$ )

$C_b$ : Conductance of the bond between the fin and the square tube W/m K

$C_p$ : Specific heat of the collector cooling medium J/kg K

$d_h$ : Hydraulic diameter (m)

F: Fin efficiency factor

F': Corrected fin efficiency

$F_R$ : Heat removal efficiency factor

GOK: Government of Kenya

G: Measured incoming solar-irradiation on the collector surface ( $W/m^2$ )

$G_T$ : Solar radiation at NOCT (Irradiance level  $800W/m^2$ , Wind velocity 1m/s, ambient temperature  $26^0C$ )

$h_{fi}$ : Heat transfer coefficient of fluid ( $W/m^2K$ )

$K_{abs}$ : Absorber thermal conductivity (m)

L: PV/T collector thickness (m)

$\dot{m}$ : Mass flow rate (Kg/s)

$\dot{Q}$ : Actual useful heat gain ( $W/m^2$ )

S: Absorbed solar energy ( $W/m^2$ )

PV/T: Photovoltaic thermal collector

TRNSYS: Transient system simulation tool

$T_c$ : Temperature of the solar cells (K)

$T_a$ : Ambient temperature (K)

$T_r$ : Reference temperature (K)  
 $T_i$ : Fluid inlet temperature  
 $U_L$ : Overall collector heat loss coefficient (W/m<sup>2</sup>K)  
W: Tube Spacing  
 $\beta$ : Temperature coefficient  
 $\tau\alpha$ : Average transmittance-absorptance of the collector  
 $\eta_t$ : PV/T thermal efficiency

# CHAPTER 1

## INTRODUCTION

### 1.1 Energy today

Over reliance on fossil fuels for production of electricity has largely contributed to widespread pollution and global warming. According to an IEA (2012) report, in 2010 41% of the greenhouse gas carbon dioxide (CO<sub>2</sub>) produced in the world was as a result of electricity generation; which is by far the largest CO<sub>2</sub> source in the world. According to IEA report of 2011, the world primary energy demand will increase by a third of the current demand between 2010 and 2035 and there will be a related CO<sub>2</sub> emission increase of 20%. The current and expected high level of CO<sub>2</sub> emission due to electric power production has necessitated a paradigm shift towards adoption of renewable energy sources, which are known to promote harmonious human-environment coexistence. Increased use of renewable energy sources would significantly diminish the demand and use of fossil based energy sources. Therefore, future potential climate change will be mitigated as a result of replacing the hazardous fossil fuels.

The main renewable energy sources include solar, wind and geothermal. Amongst these options, solar energy is quite promising given that its potential is huge but its exploitation is still low. It is estimated that 80 million kilowatts of solar energy reach the earth's surface in one second (Wu and Ren, 2012). If 1% of this energy were to be harnessed to produce electrical energy at a conversion rate of 5%, then an annual generation capacity of  $5.6 * 10^{12}$  Kwh could be realized. This is 40 times more than the current worldwide energy demand.

### 1.2 Solar energy

Solar energy can be harnessed either as heat or electric power. Heat energy is collected by solar thermal collectors. On the other hand, to harness solar energy as electric power a solar photovoltaic module is used. According to Chow (2010), in recent years a solar collector to harness both heat and electric energy simultaneously called a PV/T panel is under development.

### 1.2.1 Solar thermal collector

Thermal collectors convert the sun's rays directly to useful heat energy. Heat is generated through absorption of sun's rays by a dark coated material called an absorber. An absorber consists of a system of pipes through which a fluid flows and constantly absorbs the heat from the absorber. Finally, the heated fluid is either used directly or stored in an insulated reservoir.

Thermal collectors can be classified as either concentrating or non-concentrating. A concentrating collector has concave mirrors and lenses which focus the incoming ray of energy to a smaller surface on the thermal receiver. Therefore, the area intercepting the energy beam and that absorbing the energy beam are different. These collectors, though expensive to manufacture, they produce high temperature fluids. On the other hand, non-concentrating (flat plate) collectors have the same area for intercepting and absorbing the radiant energy. These collectors are cheap to manufacture even though their outlet fluid temperatures are relatively low as compared concentrating collectors. Owing to cost constraints and ability to collect beam and diffuse radiations, non-concentrating collectors are the most widely applied especially in household water-heating and air conditioning systems.

A non-concentrating collector consists of three main components namely the absorber plate, transparent cover (glazing plate) and an insulated box. The absorber plate's material should be highly absorptive and conductive to aid rapid heat transfer to the fins and tubes in the insulator box. It is also painted or plated in order to reduce heat loss through radiation and convection and to maximize absorption. Moreover, it is covered by a glazing plate that creates greenhouse effect to prevent the incident light photons from escaping and allow their heat energy to pass through to the absorber.

The absorber plate should be a metal that can withstand temperatures as high as 200 °C (Chow, 2010). This temperature is attained when there is no water or any fluid flowing through the tubes. Aluminium, copper or steels are the most suitable metals for the absorber plate since they cannot be destroyed by such high temperatures (Kalogirou, 2009). The absorber plate absorbs most of the sunrays incident on it since it is painted with a dark colour, most preferably black. It transmits the heat energy to the fluid even with a small temperature gradient hence minimizing heat loss. With the dark painting, the absorber plate can take up to 95% of the amount of energy

incident on it (Chow, 2010). The heat is conducted to the fluid in the collector plate tubes. These tubes are packed close together at a distance of about 10 cm. The tube spacing is made small so as to avoid heat loss when the liquid flows in the pipes. Highly conductive copper is the metal of choice for making the absorption metal sheet.

### **1.2.2 Solar Photovoltaic module**

Solar photovoltaic modules are used to convert solar irradiance to electric power. Modules absorb solar photons which knock off electrons from their shells to flow freely. This free flow of electrons constitutes current which can be collected as charge and stored in an accumulator.

The photovoltaic (PV) cell relies on the special electric properties of the element silicon. When the photovoltaic cell is exposed to light, the beam of light photons can be reflected, absorbed or passed through (Kalogirou, 2009). The absorbed portion of the light beam generates electric charges which can be collected through contacts as direct current. Electrical charges are produced as a result of transmitting the photon energy to the electrons in atoms of the semiconductor material used to make the PV cell. Consequently, this photon energy excites the electrons to escape their orbitals and become free to flow, hence constitute current flow. To induce this current flow, 'p' and 'n' type semiconductors, which correspond to the conventional positive and negative terminals respectively, are sandwiched together. These semiconductors create an electric field necessary for electron-hole flow. Thus, if a load is connected across the terminals there is electron flow which constitutes an electric current.

Most photovoltaic modules utilize a mono interface to generate current in the PV cells. However, in mono interface modules, only photons which possess energy greater than or equal to the semiconductor material's band gap energy used in the PV cells can free electrons (Kalogirou, 2009). Thus, the photovoltaic response of a mono junction cell is only limited to the photon spectrum portion whose energy is higher than the semiconductor's band gap energy as illustrated in figure (1.1). Consequently, low energy photon spectrum portion is not utilized in current generation. To overcome this challenge, Kalogirou (2009) explains that most contemporary PV modules contain various types of cells, with diverse junctions to generate current with a diverse photon energy spectrum. These PV modules are referred to as multi junction cell PV modules.

Multi junction PV modules convert more of the sun's photon spectrum to electric energy than the single junction cells hence are more efficient as compared to the former.

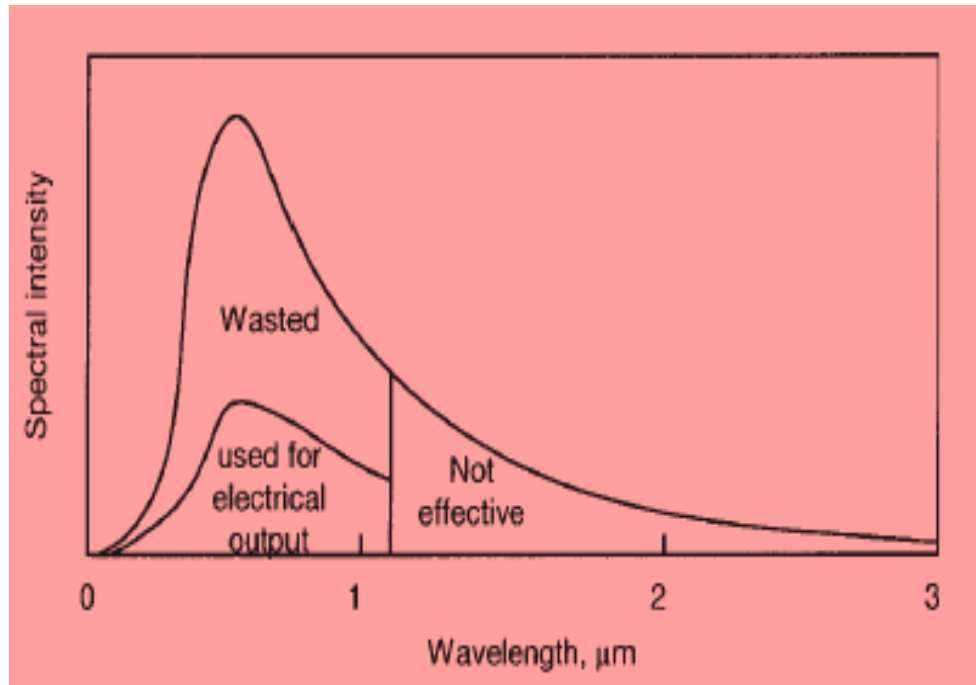


**Figure 1.1: Figure showing useful and non-useful portion of the sun's photon spectrum used to produce electric current (Helden et al., 2004).**

A variety of PV modules are commercially available in the market today. They include mono-crystalline silicon cells, polycrystalline silicon cells, amorphous silicon and thermo-photovoltaic cells. Mono-crystalline silicon cells are made from pure silicon with a single continuous crystal lattice. On the other hand, polycrystalline silicon cells are produced using numerous grains of mono-crystalline silicon. Amorphous silicon cells are quite different from the other two in that they adopt a structure of silicon atoms in a thin homogeneous layer. According to Hankins (2010), about 90% of PV production in 2008 was mono-crystalline and polycrystalline silicon. Comparing their average efficiency in service, mono-crystalline silicon cells ranks highest at 15% followed by polycrystalline cells at 12% and lastly amorphous silicon cells at 6% (Kalorigrou, 2009). However, in the laboratory setting, a cell efficiency of 25.6%, 20.8% and 21% have been recorded for mono crystalline, polycrystalline and thin film cells respectively (Fraunhofer ISE, 2016).

Several factors determine the electrical output of a solar module. These factors include; how many cells make up the module and their type, the aperture of the module, amount of solar radiation and its intensity, inclination angle, and the operation temperature (Boxwell, 2012).

Conversion efficiency of modules has been limited to about 22% in the laboratory setting (Kalogirou and Tripanagnostopoulos, 2006), thus sustained research on photovoltaic technology has always aimed at improving the conversion efficiency and reduction of production costs. This aims to make solar energy feasible to serve in a variety of applications.

### **1.2.3 Photovoltaic-thermal (PV/T) collector**

One of the primary factors that influence solar PV conversion efficiency is the PV module temperature. Chow (2010) explains that heated PV solar modules lose about 0.4% on efficiency for each degree rise in temperature. In addition, elevated temperatures of the module can cause permanent structural damage to the PV module due to persistent thermal stresses. Further, the rise in module temperature produces thermal agitation that increases the dark current and thus increases the loss of free carriers in polycrystalline modules (Malik et al., 2010). This reality of temperature effects has encouraged the development of various solar collection systems, which incorporate a heat collection system to the PV module to collect both thermal and electric energy concurrently. These systems are commonly referred to as photovoltaic-thermal (PV/T) solar collectors.

The main aim of cooling in PV/T solar collectors is to enhance the output of the photovoltaic modules by maximizing the conversion efficiency (Zondag et al., 2003). The heat extracted can be utilized in temperature utilities. This would increase the overall yield of energy per unit area of a PV module, hence saving on space compared to stand alone PV and thermal collector systems.

The PV/T system consists of a photovoltaic panel, battery, charge controller, electrical cables, thermal absorption plate, storage tank and pipes. A fluid, mainly water, flows through the pipes. Fluid flow through the pipes can be by natural convection (passive system) or forced by a pump (active system). Passive systems are normally open loop meaning that water in the solar tank flows by natural convection through the solar absorber. On the other hand, active systems are normally either closed loop or open loop. In closed loop systems, water in the solar tank is



heated through heat exchangers by the water that passes through the solar absorber. Figure (1.2) shows a schematic representation of an active PV/T system with water acting as the cooling fluid.

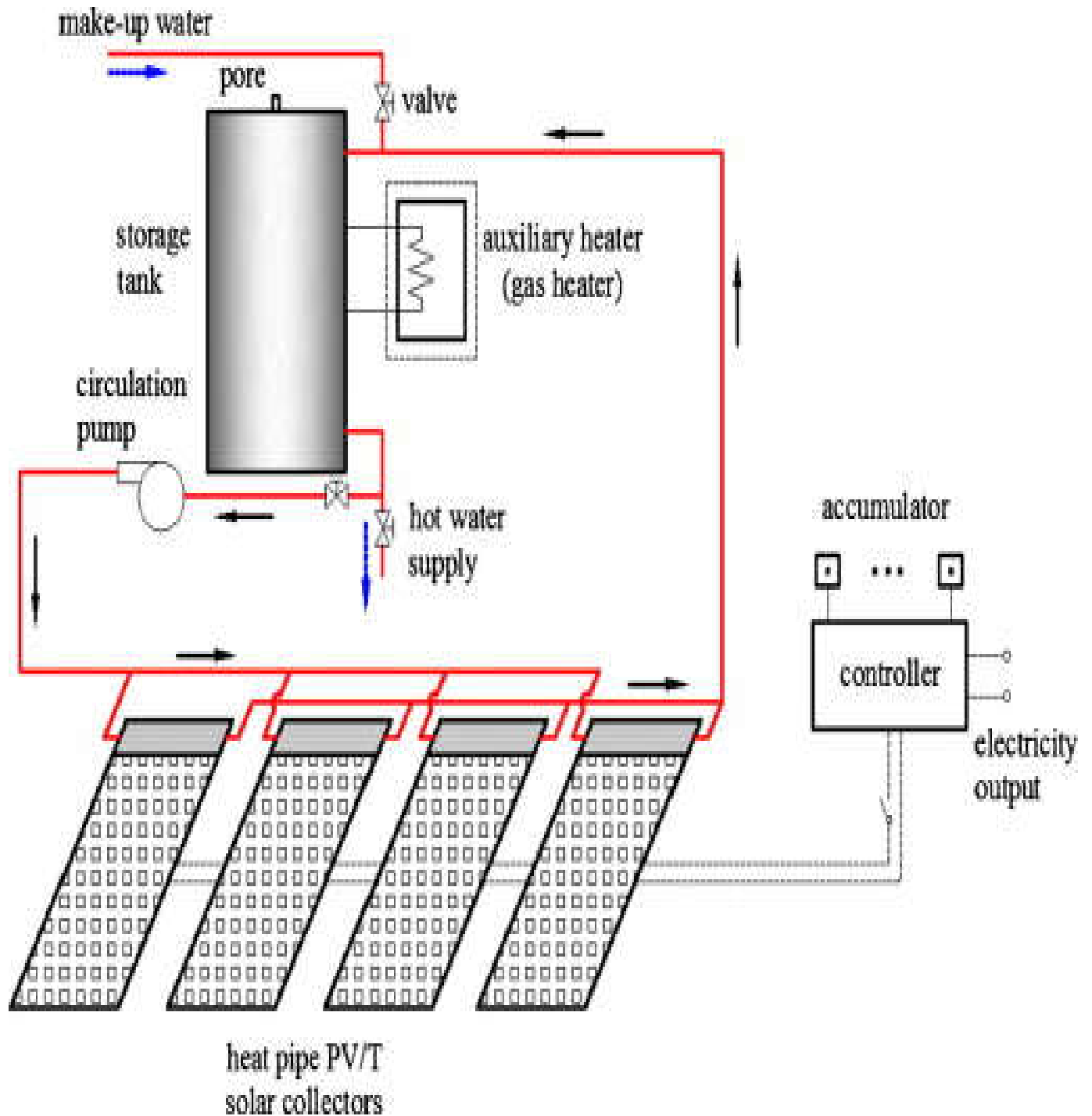


Figure 1.2: Schematic diagram of a water cooled PV/T system (Chow, 2006).

### **1.3 Research Problem**

Although considerable developments have been achieved through research in developing PV/T systems, a PV/T system that is affordable, efficient and characterized under the local tropical climatic conditions is still non-existent. Nearly all the available photovoltaic and thermal systems have been developed and characterized under climatic conditions that are not exactly the same as the local situation. Thus, the rated performance of the PV modules does not exactly agree with the actual performance when under the local conditions. This is because both amorphous and polycrystalline silicon PV plates respond differently to the prevailing climatic conditions of a given region.

The world is divided into four main climatic zones: the tropical zone, the arid sub-tropical zone, the temperate zone and the polar zone (Goat, 2012). All these zones are characterized by varying ambient temperature and solar spectrum; factors that influence solar PV and thermal systems. Research and development activities of PV/T systems have been conducted in various climatic zones. Most of these studies have been done either in Europe or Asia with a few, if any, in Kenya. Research on the PV/T system in the tropical climate, to which Kenya belongs, is therefore desirable because ambient temperatures are relatively high and the solar spectrum is favourable.

The thermal collector contributes the higher percentage of the total cost of a PV/T system (Wu and Ren, 2012). Therefore, a complementary low cost thermal collector needs to be developed to make an affordable PV/T system. According to Chow (2010), various research studies have shown that various design concepts of a thermal collector can be low cost and efficient enough to serve. Therefore, to produce a cost effective and efficient PV/T system, such design concepts need to be considered.

### **1.4 Justification**

Kenya's installed energy capacity is inadequate to serve a population of nearly 41 million people (NCPD, 2011). Currently, the rate of electrification ranges only between 15-20% at the national level with a corresponding rural electrification rate of 5-10% (Hille and Franz, 2011). Hill and Franz (2011) further explain that electricity demand is growing at the rate of between 5 and 8% per annum. Also, it is worth noting that a huge fraction of the population is based in the rural

areas which are poorly served by the national electric grid. And yet, one of the key resolutions of Kenya's Vision 2030 development blueprint is to ensure universal access to electric power (GOK, 2007). To achieve this, it is beneficial to incorporate off-grid PV systems that play an important role in pre-electrification of areas which are not covered by the national grid. Because of relatively low income levels, increased access to electric power requires that any introduced electric power systems should be economically viable to the consumers. This study targeted the low income earners especially in rural Kenya.

Kenya location near the equator assures it of solar radiation intensity 4-6 Kwh/m<sup>2</sup>/day (Hille and Franz, 2011). Therefore, this country has a huge potential to harness solar energy. To harness this energy, development of solar harnessing equipment and systems which are cost effective and efficient is necessary. Integrating PV and thermal components while taking into account cost constraints, is one way to develop cost effective and efficient systems. Hence, the development of a system of this nature whose operation characteristics under local climatic conditions is well understood is a step in the right direction.

### **1.5 Scope of the Study**

The PV/T system consists of various components which include: a PV/T collector, battery, charge controller, electrical cables, thermal absorption plate, and storage tank. The focus of the study was on the development of the PV/T collector component. Other system components were chosen based on best practice as stipulated in literature. This study was to establish the efficiency of the PV/T collector and determine whether adopting the PV/T system developed for the specific application studied can be economically viable.

### **1.6 Objectives**

The main goal of this study is to develop a liquid type flat plate PV/T system and investigate its quantitative output for a typical Kenyan family of five under local climate and weather conditions in Kenya. The specific goals are:

1. To develop a computer model of the PV/T system and determine an optimum flow rate and other performance characteristics
2. To construct and characterize the flat plate active PV/T system.
3. To quantify the economic viability of the system.

## CHAPTER 2

### LITERATURE REVIEW

#### 2.1 Introduction

A PV/T collector is a sandwich of a PV module and a thermal collector. The main purpose of sandwiching the two into a single unit is due to the benefits accrued which include higher energy per square meter of surface area, architectural uniformity on the roof, increased effective life of PV modules and lower manufacturing and installation costs. Due to these advantages, a lot of efforts in research have sought to improve this technology and make it more efficient and cost effective for wider applicability. Thus, various research activities in the last two decades have mainly focused in lowering the overall PV/T system cost and making it more efficient. This chapter outlines the major developments made in developing the PV/T collector. Further, the numerical model used to study the PV/T collector is also outlined.

#### 2.2 Major Developments of PV/T Collectors

Chow (2010) reports that major construction and operation concepts of PV/T systems have been researched and continually published for the past two decades. This author further contends that various research studies and design concepts have been evaluated to determine which combined PV-thermal collector gives the best yield. Also focus has been on different system components with the aim of realizing improved efficiency and cutting on costs of the overall system as outlined below.

There are a myriad of ways on how to sandwich a PV module and a thermal collector to make a PV/T collector. In their study, Zondag et al. (2003) evaluated the yield of different sandwich designs. The nine design ideas were grouped as two absorber, channel, free flow and sheet and tube PV/T collectors. Further, the sheet and tube collectors were such that they had zero, one or two glazing plates. In the same way, the channel PV/T collectors were sub-divided into channel above the PV, channel below a transparent PV and channel below an opaque PV. From experimental analysis, it was established that the PV/T collector with no glazing plate and that of sheet and tube gave the worst performance. However, the sheet and tube collector with one or

two glazing plates showed a higher efficiency as compared to that without a glazing plate. It was also observed that the channel collector, the free flow collector and the two absorber plate collector have a higher efficiency than the tube and sheet collectors. The channel PV/T collectors were observed to be the best. Although the channel below transparent PV design concept was observed to be the most efficient, PV on sheet and tube design is easier to manufacture and its efficiency is only 2% less than the latter. Thus, PV on sheet and tube design was identified as the best alternative.

The fluid flow configuration influences the combined efficiency of a PV/T system. Ibrahim et al. (2009) investigated seven different fluid flow configurations within a flat plate PV/T collector. The design concept applied in the research is that of PV on sheet and tube. In their research, various design configurations were simulated to determine the configuration that maximizes both thermal and electricity yields. Various design parameters were used during analysis and they include radiation intensity, ambient temperature and fluid flow rate. The design configurations studied were classified as serpentine, modified serpentine oscillatory, spiral, parallel serpentine, direct and web. From the simulations, spiral gave the highest output temperature followed by modified serpentine-parallel, parallel serpentine, direct, web, oscillatory and serpentine configuration respectively. With a 50.12% thermal efficiency and an 11.98% PV cell efficiency, the spiral configuration was concluded to be the best. The study also observed that the spacing between the pipe runs play a pivotal role in a design configuration, and thus zero tolerance gap between pipes results in a more efficient PV/T collector.

A PV/T system can be manufactured from either polycrystalline silicon or amorphous silicon PV modules. To establish the suitability of either of the two, Kalogirou and Tripanagnostopoulos (2006) constructed, modelled and simulated PV/T systems comprising both types of PV modules. The research featured a small thermosyphonic system, suitable for domestic application and a large active system, applicable in large scale operations. The results proved that polycrystalline PV modules show higher electrical efficiency than amorphous PV modules even though their thermal efficiency is lower. In comparison with a non-hybrid PV system, it was established that 38% more electrical energy is produced by the non-hybrid PV system as compared to the PV/T system. Additionally, since the results were given for three different

locations; Nicosia, Athens and Madison, it was established that the economics of the system give better figures in areas with higher availability of solar radiation.

A PV/T collector performance does not only depend on its inherent parameters, but also on the prevailing climatic conditions in a given location. Nualboonrueng et al. (2012) studied outdoor performance of PV/T collectors in the climate of Bangkok, a tropical region. Tests were carried out on both multi-crystalline and amorphous silicon PV/T plates in a climate replicating the energy consumption behaviour of Thai medium-size families. The study established that multi-crystalline and amorphous PV/T collectors show nearly equal thermal performance, but polycrystalline PV/T collectors show about 1.2 times better electrical performance than amorphous PV/T collectors. It also proved that approximately 50% of sunlight was converted to heat energy with corresponding 4-5% conversion efficiency to electrical energy. The study established that high ambient temperature in Bangkok led to dismal electrical efficiency of the PV/T collectors. In comparison to a study carried out in Cyprus by Nualboonrueng et al. (2012), it was noted that thermal performance is better in Bangkok whereas electrical efficiency is better in Cyprus. The study concluded that PV/T collectors are largely affected by ambient temperature differences.

The thermal contact between the solar module and the thermal absorber is a major factor in determining heat absorption efficiency by the heat transfer fluid. A study by Zakherchenko et al. (2004) established that commercial PV modules should not be used directly to produce PV/T collectors. The argument was that commercially available PV modules usually have an embedded laminate which hinders proper thermal contact between the PV module and the thermal absorber. In another study, Wei He et al. (2006) also showed that proper thermal contact between the thermal absorber and the PV module significantly improves the overall PV/T efficiency. Both researchers also concluded that a highly effective fin of the heat exchanger boosts the overall efficiency of the PV/T collector.

Residential buildings rooftops usually host PV/T system collectors. To investigate actual behavior when in service, Ji et al. (2003) installed a 40 m<sup>2</sup> PV/T collector on residential building's façade in Hong Kong. Under similar weather conditions, a PV/T collector made from

thin film silicon gave a thermal efficiency of 48% whereas a PV/T collector made from crystalline silicon gave a thermal efficiency of 43%.

The geometric flow rate of the fluid through the absorber tubes greatly influences the overall performance of a PV/T system. In his research to determine the effect of flow rate on efficiency, Chow (2010) established that when flow rate in the absorber tube increases from 0.001 to 0.0075 kg/s both thermal and electrical efficiencies increase. Further, Garg and Agarwal (1995) used the finite difference method to study the PV/T system with various solar cell areas and flow rates. They established that for maximum thermal efficiency, the optimum flow rate is 0.03 kg/s. It was also shown that at this optimum flow rate for maximum thermal efficiency, electrical efficiency increased and was at a maximum when the solar insolation was at a maximum.

### **2.3 Photovoltaic-thermal collector characteristics**

Analyzing a solar energy system is a complex endeavor given the various predictable and unpredictable parameters. Modelling and simulation procedures are commonly used to aid the design process since they can give an optimum model before fabricating the prototype. Florschuetz (1979) published the first PV/T collector mathematical model. This first model was achieved by modifying Hottel and Willier(1958) flat plate thermal collector analytical model. The main aim was to be able to accurately determine the heat removal factor ( $F_R$ ) and the overall loss coefficient ( $U_L$ ) of the PV/T collector.

The performance of PV/T collectors is depicted by a combination of thermal and electrical efficiency according to Florschuetz (1979) and is given by equation (1).

$$\eta = \eta_t + \eta_e \quad (1)$$

where  $\eta_t$  and  $\eta_e$  represent thermal and electrical efficiencies respectively.

Various design parameters and operation conditions affect the thermal performance of the PV/T. During simulation studies, analysis is based on diverse solar radiation, ambient temperature and flow rate configurations. A major assumption during the simulation studies is that the PV/T collector is like a flat plate thermal collector with a single glass glazing plate. Therefore, the derivation of the PV/T unit efficiency parameters is based on already known Hottel and Whillier

(1958) equations. Equations (2) to (11) outline how to determine heat removal factor ( $F_R$ ) and the overall loss coefficient ( $U_L$ ) of the PV/T collector which are essential in determining the thermal ( $\eta_t$ ) and electrical ( $\eta_e$ ) efficiencies.

According to Hottel and Whillier(1958), for a flat plate solar collector the thermal efficiency ( $\eta_t$ ) is given by equation (2).

$$\eta_t = \frac{\text{Heat gain by the fluid through the absorber tubes (Q)}}{\text{Measured incoming solar radiation on the collector surface (G)}} \quad (2)$$

For water flowing through the absorber tubes of the system, the rate of heat gain ( $\dot{Q}$ ) by the water is given by equation (3)

$$\dot{Q} = \dot{m}C_p(T_o - T_i) \quad (3)$$

where  $\dot{m}$  is the mass flow rate of water,  $C_p$  is the specific heat capacity of water,  $T_o$  is the water outlet temperature and  $T_i$  is the water inlet temperature.

According to Ibrahim et al. (2009), the rate of heat gain is also given by equation (4).

$$\dot{Q} = A_C F_R [S - U_L(T_i - T_a)] \quad (4)$$

where  $A_C$  is a function of the collector area,  $F_R$  the heat removal efficiency factor,  $S$  is the absorbed solar energy, and  $U_L$  is the overall collector heat loss coefficient.

The absorbed solar energy ( $S$ ) is given by equation (5).

$$S = (\tau\alpha)_{PV} G_T \quad (5)$$

where  $(\tau\alpha)_{PV}$  is the average transmittance-absorptance of the collector and  $G_T$  is the solar radiation at NOCT.

According to Florschuetz (1979), the heat removal efficiency factor ( $F_R$ ) and the corrected fin efficiency ( $F'$ ) are given by equation (6) and (7) respectively.



$$F_R = \frac{\dot{m}C_p}{A_C U_L} \left\{ 1 - \exp \left[ -\frac{A_C U_L F'}{\dot{m} C_p} \right] \right\} \quad (6)$$

$$F' = \left[ \frac{1}{U_L (d_h + (W - d_h)F)} \right] + \frac{1}{C b_{PV}} + \frac{1}{2(a+b)_{h_{fi}}} \quad (7)$$

where  $d_h$  is the hydraulic diameter,  $W$  is the tube spacing,  $C b_{PV}$  is the conductance of the bond between the fin and square tube,  $(a + b)_{h_{fi}}$  is the heat transfer coefficient of the fluid and  $F$  is the efficiency factor and is calculated using equation (8).

$$F = \frac{\tanh \left[ m \left( \frac{w - d_h}{2} \right) \right]}{\sqrt{m \left( \frac{w - d_h}{2} \right)}} \quad (8)$$

$$\text{where } m = \sqrt{\frac{U_L}{K_{abs} L_{abs} + K_{PV} L_{PV}}} \quad (9)$$

where  $K_{abs}$  is the absorber thermal conductivity,  $L_{abs}$  is the PV/T collector thickness,  $K_{PV}$  the photovoltaic thermal conductivity and  $L_{PV}$  is the PVT collector thickness.

Equation (10) gives the useful heat gain by the PV/T solar collector.

By rearranging equation (2) equation (10) is arrived at which gives the thermal efficiency of the PV/T collector.

$$\eta_t = F_R (\tau\alpha)_{PV} - F_R + U_L \frac{T_i - T_a}{G_T} \quad (10)$$

Electrical efficiency ( $\eta_e$ ) of the PV/T collector is determined using Tiwari et al. (2006) published equation of temperature dependence of electrical efficiency outlined as equation (11).

$$\eta_e = \eta_r [1 - \beta(T_C - T_r)] \quad (11)$$

where  $T_r$  is the reference temperature,  $\beta$  is the Temperature coefficient,  $T_C$  is the temperature of the solar cells and  $\eta_r$  is the reference efficiency of the PV module (0.12).

## CHAPTER 3

### METHODOLOGY

#### 3.0 Introduction

This chapter outlines the methodology that was applied during the study. First, the steps followed in coming up with the model PV/T collector are described and then the simulation procedure is described. Second, the construction details of the PV/T system are described and the experimental procedures involved in characterizing the system are explained.

#### 3.1 Modelling and simulation

Modelling is an activity aimed at visualizing a particular phenomenon which does not exist by relating to existing knowledge. For the sake of this study, to visualize the PV/T system, a set of the system requirements were first determined. Together with known parameters of the system, a model system was built in a virtual computer environment to investigate its operation characteristics. The conditions set in the virtual environment correlate directly to the physical phenomenon in which the actual PV/T system was going to operate.

##### 3.1.1 Determining the demand from the system

One of the major requirements of a PV/T system is to meet the expected demand of heat and electrical energy. Thus, before modelling and simulation, it was crucial to fix the expected demand from the PV/T as a system requirement. Consequently, both the electrical and thermal energy demand from the system was approximated. Tables 1 and 2 give a step by step approach used to approximate the expected demand from the PV/T system. The approximated demand capacities guided the modelling and simulation process in ensuring that the chosen model to be constructed meets the expected demand.

Using the expected electrical energy demand, the size (wattage) of the required solar panel was determined. Using the wattage determined, the solar panel was selected from a range of solar panels available in the Kenyan market. The major factor used in settling for one of the panels is

the aperture area exposed such that the one exposing the maximum area was chosen. The aperture area was important in ensuring maximum heat collection by the thermal absorber plate.

**Table 1: Daily load energy demand for a typical Kenyan family of five**

	Number of appliances	Power rating (W)	Voltage (V)	Hours of usage/day	Energy use (Wh)
DC booster Pump for water circulation in the system	1	50	12	5	250
Lighting bulbs	5	5	12	3	75
Television (Based on Sony 24” 22BX310 Widescreen LCD TV )	1	50	110~240	3	150
Cell phone recharging	5	2	100~240	2	20
<b>Total daily system energy demand</b>					<b>495</b>
Adjustment for losses (Inefficiencies in cables, modules, batteries, charge controllers and inverters )	10 % of subtotal				49.5
<b>Total daily system energy demand + losses</b>					<b>544.5</b>

To determine the solar panel size (wattage) the operation system voltage was selected as 12V. Using the system voltage selected and the daily load energy demand from table 1, the daily system charge requirement was calculated as follows:

$$\begin{aligned} \text{Daily system charge requirement} &= \frac{\text{Total daily system energy demand} + \text{Losses(Wh)}}{\text{System voltage (V)}} \\ &= \frac{544.5\text{Wh}}{12\text{V}} = 43.375\text{Ah} \end{aligned}$$

43.375 Ah is the charge in amp-hours that the module has to produce each day to meet the load requirements.

To determine the system design charging current, one must know the daily solar insolation value of the physical environment in which the PV/T system is to operate. For this study, the daily solar insolation value for a site near the University of Nairobi is given as 5.5 Peak Sun Hours (PSH) from the data outlined in appendix D (Hilland Franz, 2011). Thus, the system design charging current was calculated as follows

$$\text{system design charging current} = \frac{\text{Daily system charge requirement}}{\text{Design solar insolation value}} = \frac{43.375\text{Ah}}{5.5\text{PSH}} = 8.25 \text{ A}$$

8.25 A is the charging current the module should produce under normal operating conditions.

Alternatively, the required module can be determined by calculating the required module input in terms of wattage (Wu and Ren, 2012).

$$\begin{aligned} \text{Required solar panel input} &= \frac{\text{Total daily system energy demand} + \text{Losses (Wh)}}{\text{Design solar insolation value}} \\ &= \frac{544.5\text{Wh}}{5.5\text{PSH}} = 99 \text{ W} \end{aligned}$$

From the required solar panel input, a solar panel that will generate 99 watts per hour is needed.

A 100 W polycrystalline solar panel of Tianwei Yingli New Energy Resources Company, YLP100P-17b was chosen for the system. The parameters for the chosen panel are as listed below:

- Power 100 W;
- Rated voltage 18.5 V;
- Rated current is 5.41 A;
- Open circuit voltage is 22.9 V;
- Short circuit current is 5.74 A
- Maximum system Voltage is 600 V.

From table 2, the Volumetric daily water demand,  $V = 140 \text{ L} = 0.14 \text{ m}^3/\text{day}$ .

Using the volumetric daily water demand, the hot water energy demand (D) for the family of five can be determined. Assuming cold mains water supply temperature ( $T_i$ ) of 20 °C and water distribution temperature ( $T_o$ ) of 45 °C, the hot water energy demand is determined as follows

$$D = V\rho C_p(T_o - T_i)$$

Where  $\rho$  is water density and  $C_p$  is the specific heat capacity of water.

Therefore,  $D = 0.14 \times 1000 \times 4.18 \times (45 - 20) = 14630 \text{ kJ/day} = \mathbf{14.63 \text{ MJ/day}}$

**Table 2: Estimate of hot water required for a five member Kenyan family**

	Typical Kenyan family water consumption		
	Average litres per use	Frequency per day	Litres per day
Showers	10	5	50
Dish wash	20	3	60
Food preparation	10	3	30
<b>Total</b>			<b>140</b>

The thermal collector, whose area has been fixed by the PV module chosen, has to produce **14.63 mJ** of energy per day in order to meet the expected demand. Thus, to determine whether it is possible to generate this thermal load required, detailed simulation which took into account the available solar radiation and other parameters and performance characteristics of the collector components was conducted on a model developed in a transient system simulation tool (TRNSYS).

To simulate the PV/T system in TRNSYS, an hourly consumption profile is required. Though the hot water demand is never uniform and is subject to daily variations, the consumption profile gives a repetitive load for the sake of making practical sense. Figure (3.1) gives an assumed consumption load for the 140litres of the hot water demanded by the design family of five within 24 hours.

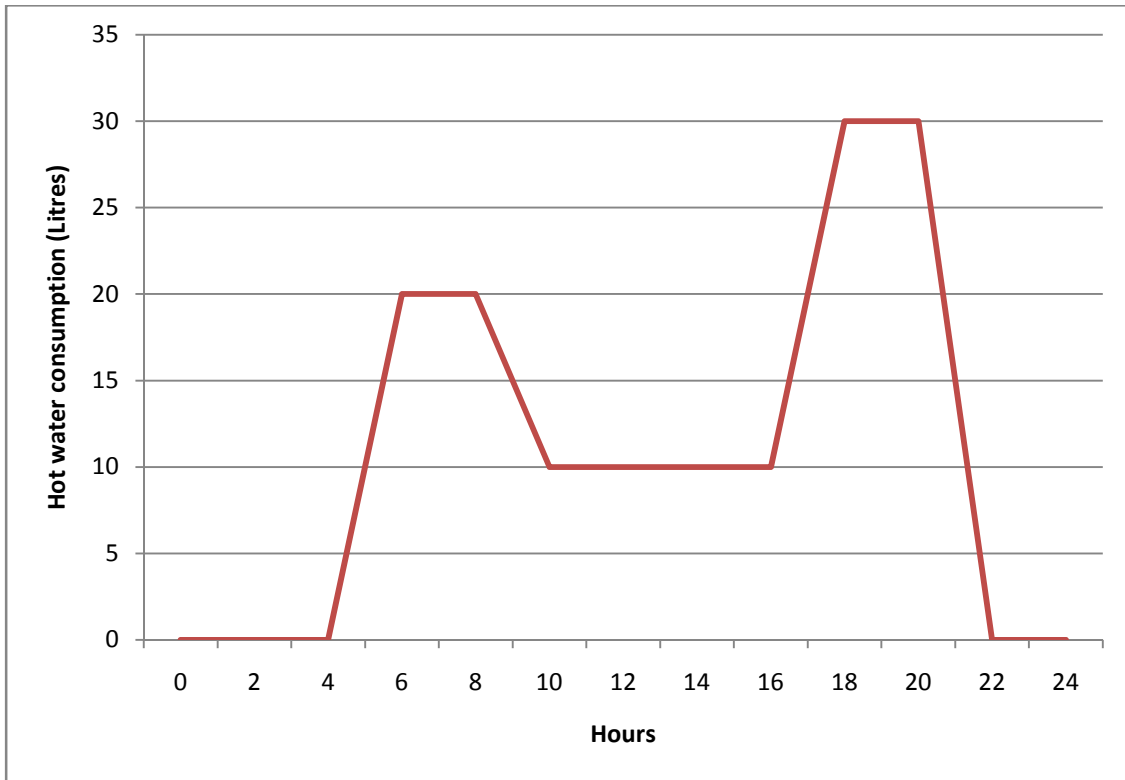


**Figure 3.1: Hot water consumption profile for a family of five**

### **3.1.2 Modelling Approach**

A PV/T system model conceptualized was built in the modelling and simulation software TRNSYS. TRNSYS is graphically based simulation tool used for the study of non-static systems. Mathematical expressions of various PV/T system components are in-built in the simulation tool. Therefore, to build the conceptualized model, relevant mathematical expressions representing individual system components were identified. An information flow diagram was then constructed which shows flow of information between various individual components of the system. An information flow diagram for the model PV/T system constructed is shown in figure (3.2). The constant parameters were provided into the system through the user interface since they were readily available from the various components identified (table 3). Weather data conditions were provided through typical meteorological year (TMY) conditions for Nairobi.

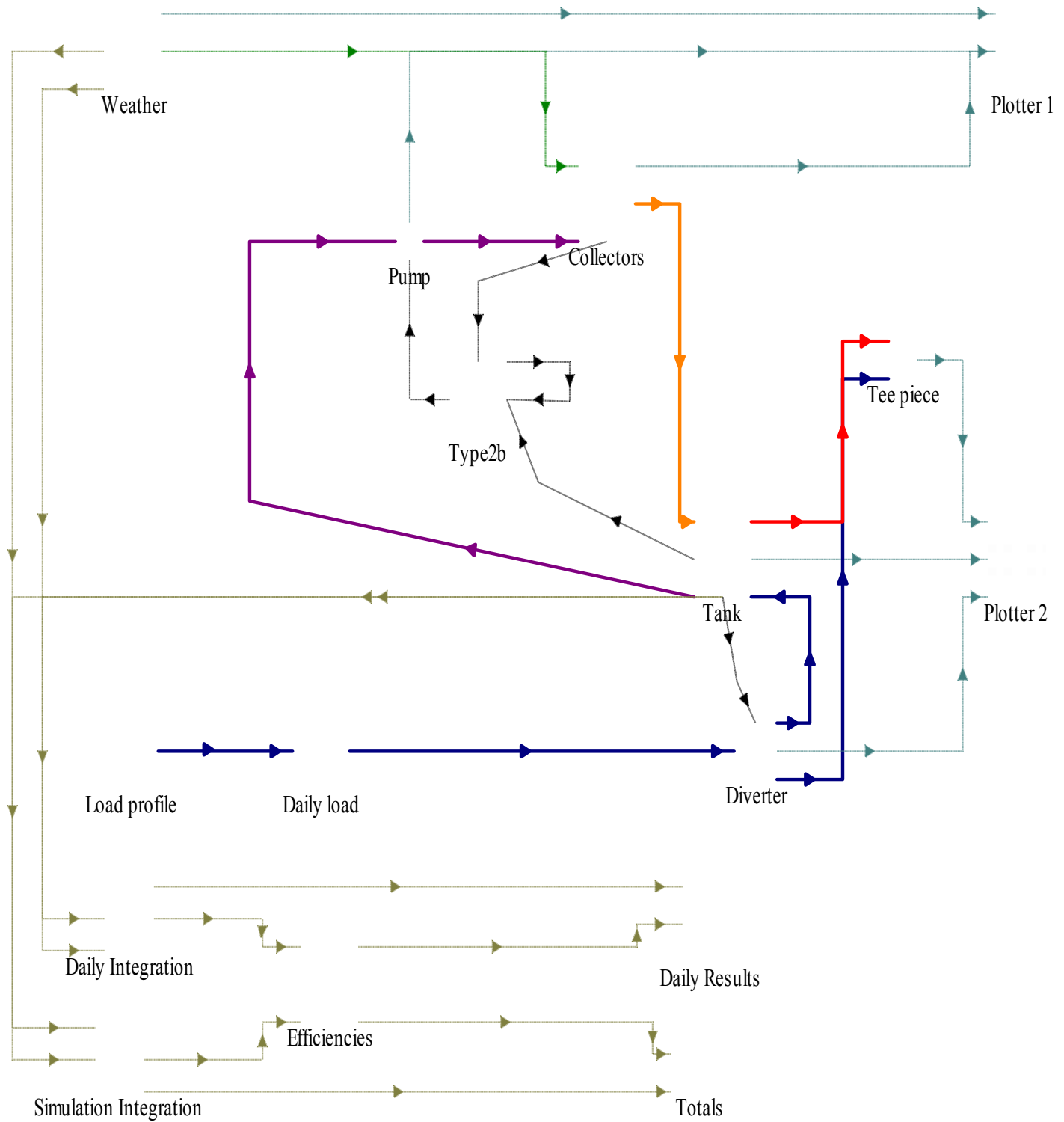


**Figure 3.2: Information flow diagram for the model constructed in TRNSYS**

**Table 3: Parameters for the simulation model**

Description	Value	Units
Number of cover glass (N)	1	
Ambient temperature ( $T_a$ )	293	K
Inlet fluid temperature ( $T_i$ )	293	K
Emittance of plate ( $\epsilon_p$ )	0.95	
Emittance of glass ( $\epsilon_g$ )	0.88	
Insulation Conductivity ( $K_e$ )	0.04	W/mK
Edge insulation Thickness ( $L_{edge}$ )	0.025	m
Collector's Perimeter (p)	4.872	m
Photovoltaic-thermal collector thickness ( $L_{pvt}$ )	0.02	m
Absorber thickness ( $L_{abs}$ )	0.002	m
Tube inside diameter (D)	0.01	m
Back insulation thickness ( $L_b$ )	0.05	m
Collector's Surface ( $A_c$ )	1.32	m <sup>2</sup>
Back insulation thermal conductivity ( $K_b$ )	0.04	W/mK
Absorber thermal conductivity ( $K_{abs}$ )	385	W/mK
Photovoltaic laminate thermal conductivity ( $K_{pv}$ )	84	W/mK
Tube Spacing (W)	0.095	m
Heat transfer coefficient between cell absorber ( $h_{ca}$ )	45	W/m <sup>2</sup> K
Heat transfer coefficient inside tube ( $h_{ti}$ )	300	w/m <sup>2</sup> K

### 3.2 Experimental characterization

The PV/T system was constructed such that its parameters merged as close as possible to the model simulated. The system was mounted in an uncontrolled meteorological environment within the Institute of Nuclear Science and Technology, University of Nairobi. This is to ensure that the conditions correlate directly to the virtual phenomenon in which the model PV/T system was simulated.



### 3.2.1 Layout of the constructed PV/T system

A commercial PV module available in the Kenyan market was used as a heat absorber of the system. The PV on sheet and tube sandwiching configuration was used since it is easy to construct according to Zondag et al. (2003). The PV panel's top surface was made of glass whereas the back surface was made of a polymer sheet. Wire gauze was adhered to the back surface of the panel using thermal glue. The wire gauze was pre-formed into six parallel circular channels onto which circular copper tubes were attached. On top of the copper tubes was a 30 mm thick Styrofoam sheet to prevent heat loss. The parallel flow design configuration was used in this study since it was reported by Ibrahim et al. (2009) to be efficient for thermal collection in their simulations of various PV/T configurations when ease of construction is considered.

Characteristics of the PV/T collector that was constructed include;

- a) Circulation line: hollow copper tubes 10 mm diameter were used. Stainless steel wire gauze with a darkened surface was closely fixed on the back of the PV panel (Figure 3.3).
- b) Insulation: Insulation adopts Styrofoam, of 30 mm thickness.
- c) Solar module: Rated power 100 W; rated voltage 18.5 V; rated current 5.41 A; open circuit voltage 22.9 V; Short circuit current 5.74A and maximum system voltage 600 V. Panel dimensions are 657mm \* 1007 mm\*23 mm giving an effective area  $A_c=0.01522\text{m}^2$
- d) Major method of joining: Screws and Adhesives



**Figure 3.3: Water circulation line behind the PV module**

Figure (3.4) is a schematic diagram of the complete flat plate PV/T system and figure (3.5) is a photograph of the experimental rig.

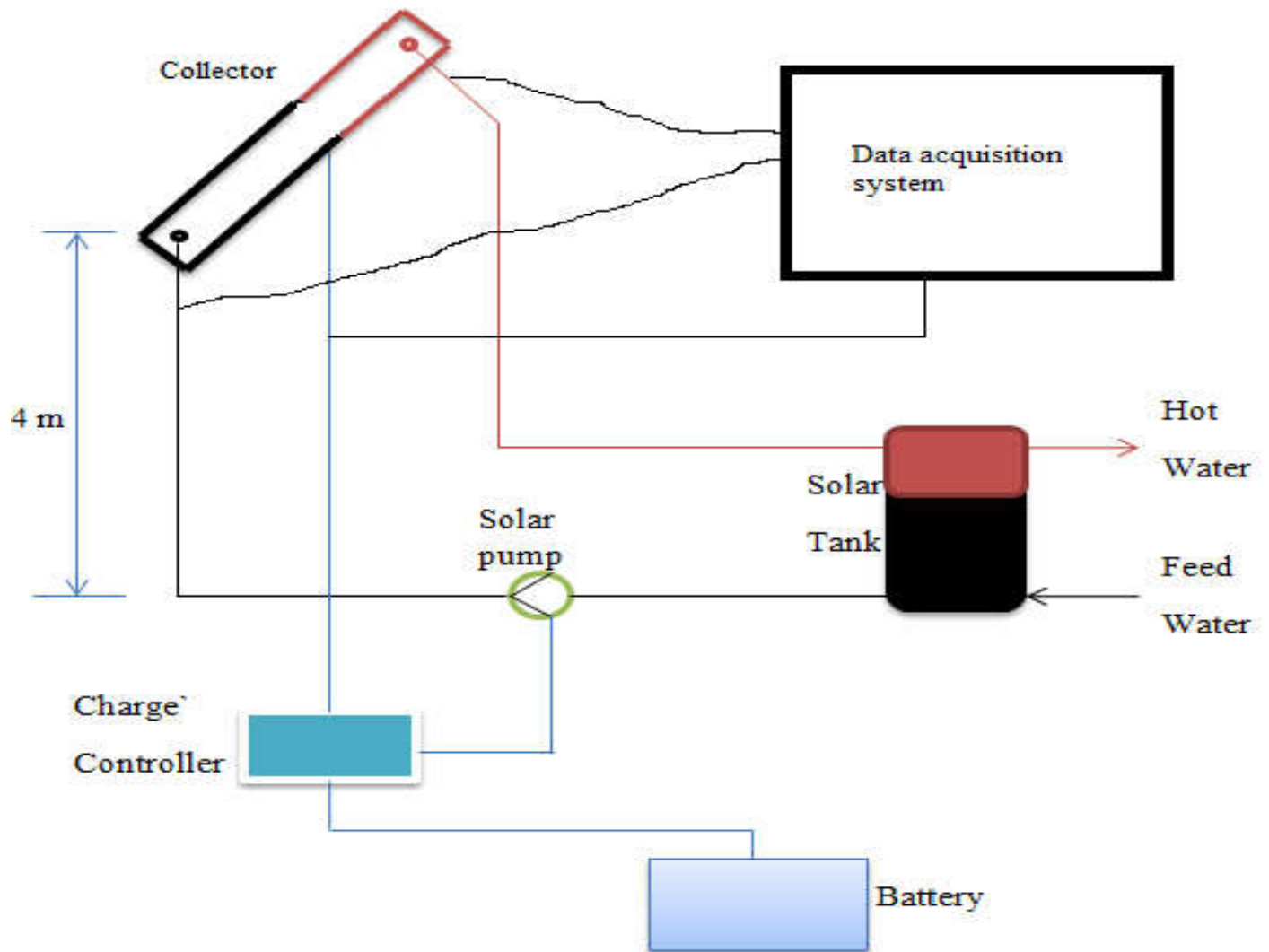
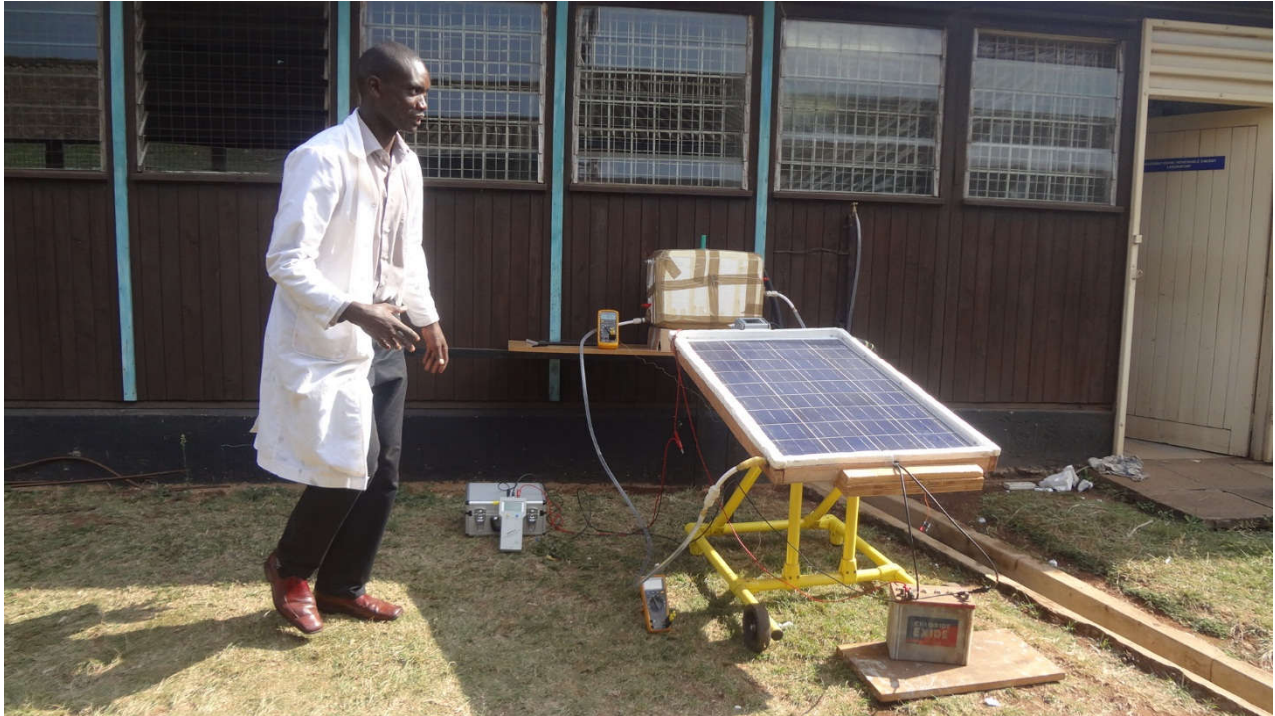


Figure 3.4: Schematic representation of the PV/T system under study



**Figure 3.5: Experimental rig**

When the PV module cells are exposed to the sun's rays, the high energy photon spectrum generates electricity whereas the low energy photon spectrum is absorbed causing the thermal absorber to increase its temperature. Due to a temperature gradient between the absorber tubes and the water passing through the tubes, the water gains heat energy hence increasing its temperature. The water flows at an optimum rate of 25 L/hour which maximizes both electrical and thermal energy.

The electricity produced by the PV panel is stored in a deep cycle gel battery through a 10 A charge controller. Two 10 W lamps were used to discharge the battery overnight. This is because if the batteries are fully charged during tests, it would affect the current production from irradiation.

### **3.2.2 Measurements**

Solar radiation was measured by an irradiance sensor Si-01TC-T placed at the same level and in parallel situation as the PV/T collector surface as shown in figure (3.6).

The current and voltage characteristics of the PV panel were monitored using the Mini-KLA (figure 3.7). The Mini-KLA is a complete measuring system for taking I-V curves of PV modules with open circuit voltages of up to 120 V and short circuit currents of up to 8 A. Global irradiance and module temperature are measured at the same time, so that all relevant parameters for calculation on STC data are taken.

High accuracy thermocouples were mounted on three monitor points. The three monitor points are used to measure the inlet and outlet temperature of the water as well as the internal cavity temperature of the panel surface. Figure (3.8) shows the attachment of the thermocouple to a monitor point.

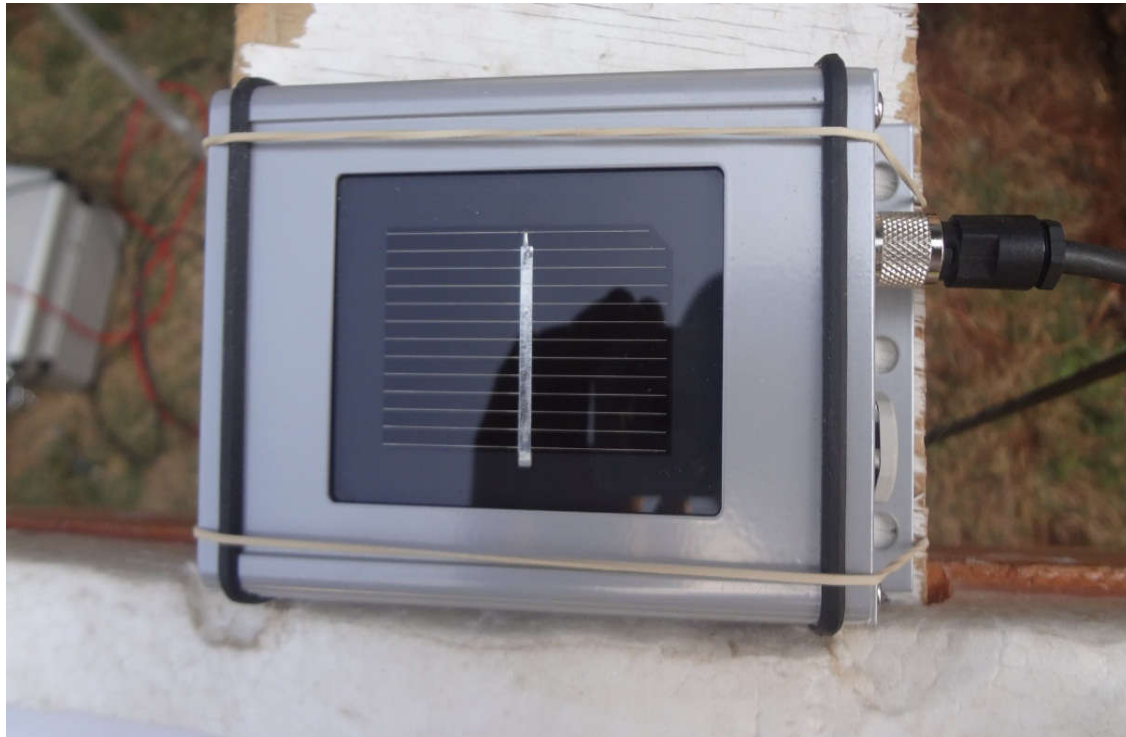


**Figure 3.6: Irradiance sensor type Si-01TC-T used to measure solar radiation**





**Figure 3.7: Measuring system for taking I-V curve of the PV module (Mini-KLA)**

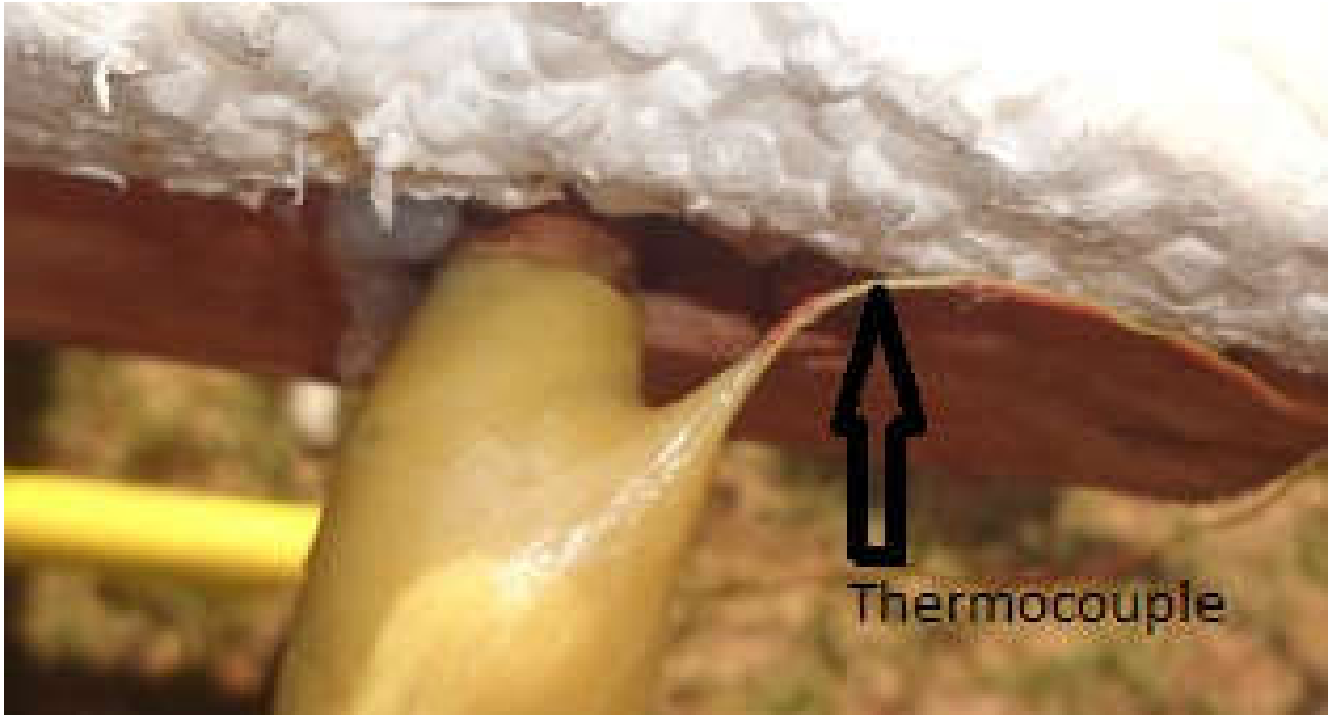


**Figure 3.8: Thermocouple attached to a monitor code**

### 3.2.3 Experimental Procedure

The performance of the PV/T system was monitored during the month of August 2014. The following experimental procedure was followed

- a) The irradiance sensor Si-01TC-T was placed at the same level and in parallel situation as the PV/T collector surface while ensuring there are no shading effects on the sensor.
- b) The Si-01TC-T was connected to the Mini-KLA using the 4-pole plugged cable so as to measure and store irradiance and temperature for every I-V curve taken.
- c) The PV module was connected to the Mini-KLA using cables which Plug into the 4 mm bananas of the Mini-KLA. The black pole of the Mini-KLA was connected to the minus pole of the PV while the red pole of the Mini-KLA was connected to the plus-pole of the PV.
- d) Thermocouples were properly attached to their respective monitor codes and each thermocouple was connected to a meter.
- e) The water flow rate through the PV/T panel was set to 25 L/h. This was achieved by using a graduated beaker and a stop watch.
- f) Data collection started after 30 minutes of setting the experimental rig. Data was collected after intervals of one hour between 8.30 am and 5.30 pm.

## CHAPTER 4

### RESULTS AND DISCUSSION

#### 4.1 Simulation Results and analysis

The simulation results reported in this chapter include the overall efficiency of the system, the total amount of energy collected from the system and the water temperatures from the system. The results of August 27<sup>th</sup> 2014 were randomly chosen to plot graphs to correlate various parameters of the PV/T system

##### 4.1.1 Optimization of the water flow rate

The rate at which water flows through the PV/T collector tubes is one of the determinants of how much heat energy can be collected from the PV panel. Therefore, there is a need to determine an optimum flow rate, which maximizes both the electrical and thermal energy collected. This design flow rate is very crucial in ensuring maximum overall efficiency of the PV/T system designed.

To determine the optimum flow rate, the annual energy output of the TRNSYS model was determined for various flow rates. The annual output of both electrical and thermal energy for various flow rates is shown in table 4.

The optimum flow rate was determined by plotting the water flow rate against the total system energy output as shown in figure (4.1). The optimum flow rate corresponds to 25 L/h. This is the flow rate value, which maximizes the energy collected from the system. The total system energy collected increases rapidly and peaks at a flow rate of 25 L/h before decreasing. The decrease in total system energy collected after attaining a flow rate of 25 L/h is approximately linear.

It was noted that the thermal energy collected increases steadily with increase in flow rate and peaks at 25 L/h and then drops subsequently. Even though the electrical energy collected increases steadily with increased flow rate, it is vital to note that the value increases dismally

after a flow rate of 25 L/h is attained. The increase in electrical energy production can be attributed to the panel working at low temperatures.

**Table 4: Annual output of electrical and thermal energy for various water flow rates**

Water flow rate (L/h)	Electrical Energy output (GJ)	Thermal Energy output (GJ)	Total energy output (GJ) (Electrical energy + Thermal energy)
0	1.332	0	1.332
15	1.568	2.567	4.135
25	2.544	5.678	8.222
50	2.683	3.432	6.115
100	2.765	1.678	4.443
150	2.781	0	2.781

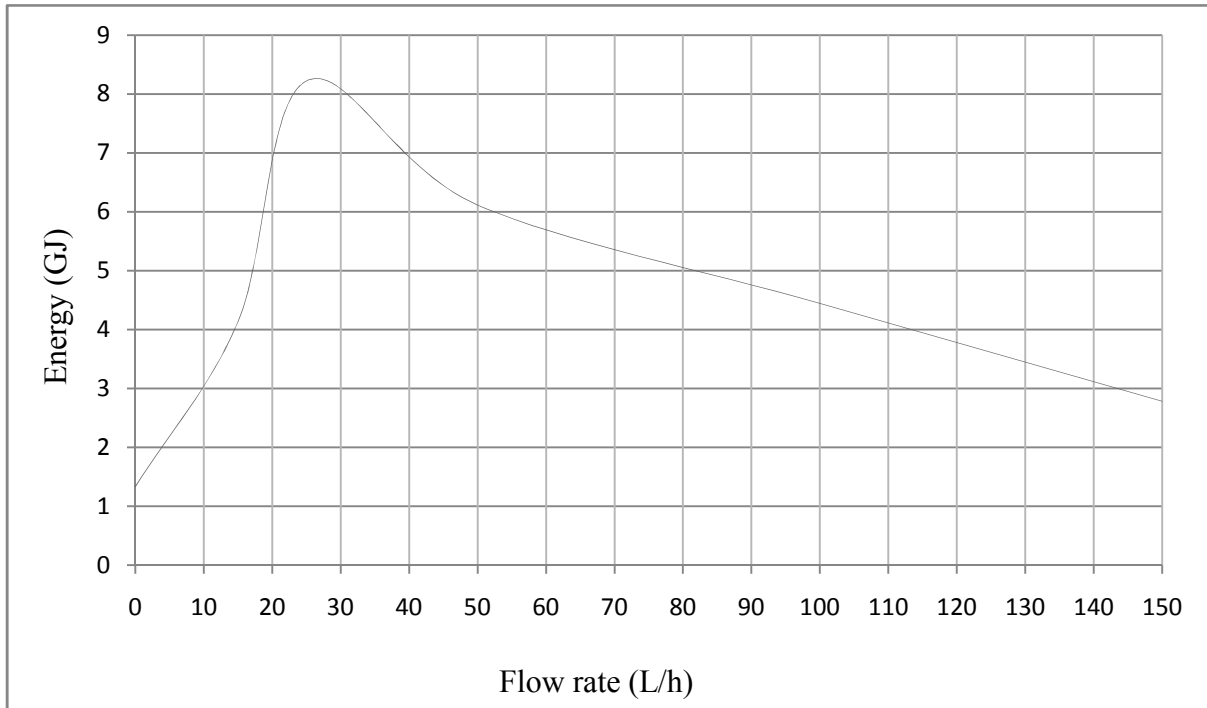


**Figure 4.1: Graph of water flow rate through the PV/Tcollector as a function of total system output (TRNSYS model)**



### 4.1.2 Hourly performance of the system

The results for August 27, 2014 were used to illustrate the performance of the PV/T model. Figure (4.2) shows performance of the system on an hourly basis in terms of thermal and electrical output. The optimum flow rate of 25 L/h was used.

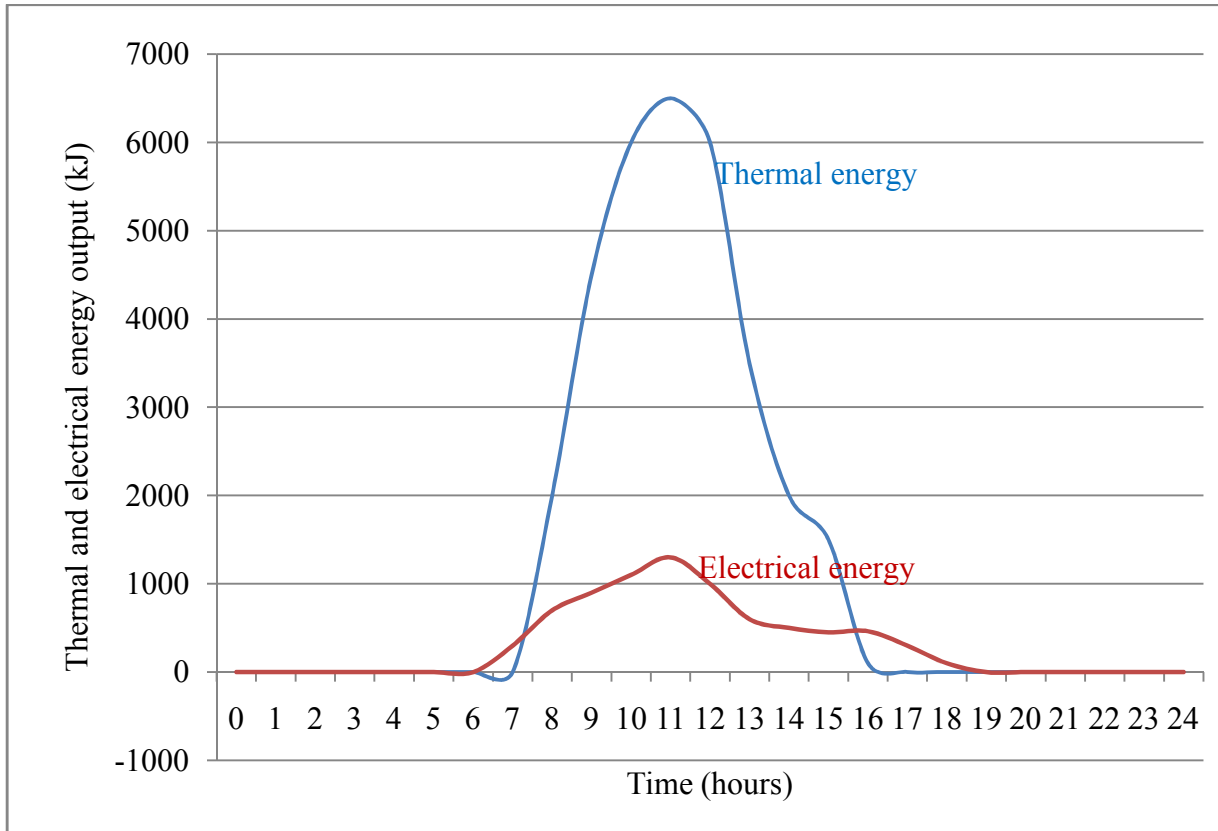
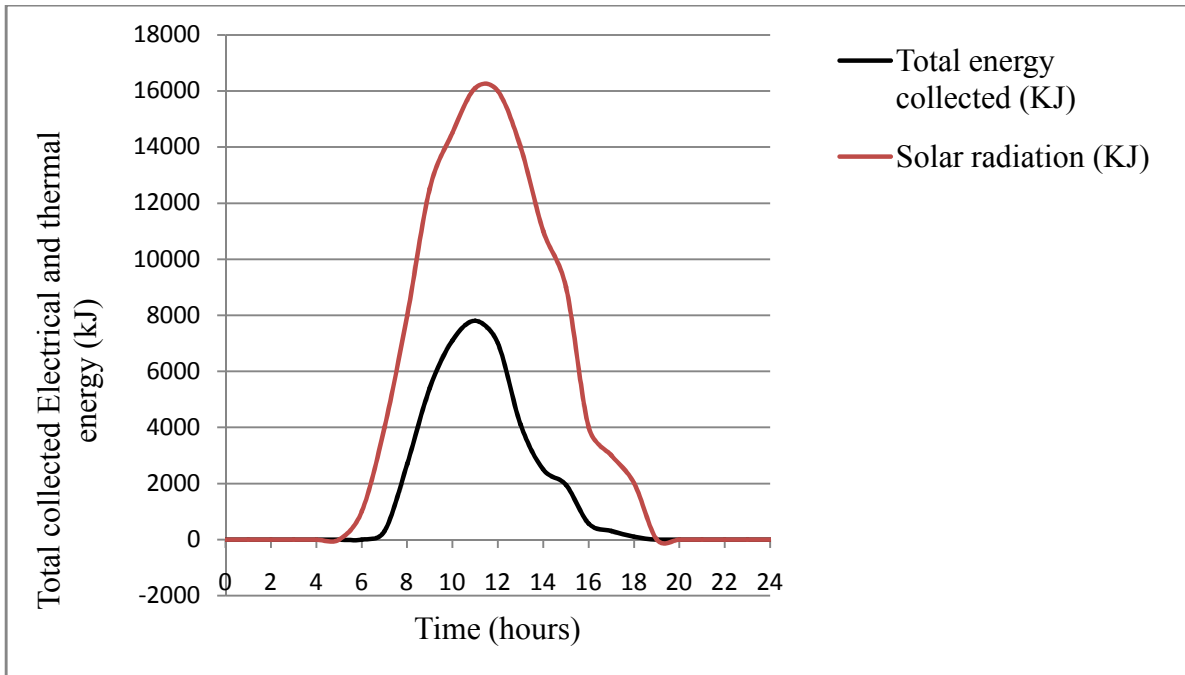


**Figure 4.2: Electrical and thermal energy output from the TRNSYS Model in a period of 24 hours**

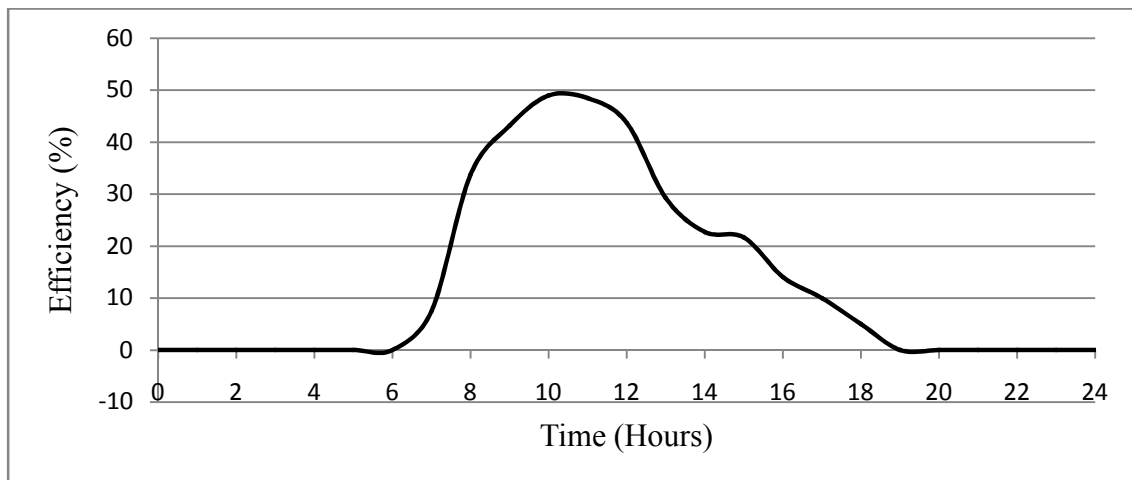
Figure 4.3 shows the performance of the system on 27<sup>th</sup> August in relation to the solar radiation. It was observed that the energy collected is directly proportional to the solar radiation since the total energy collected curve and the solar radiation curve have a similar pattern.

Figure (4.4) shows the performance of the system on 27<sup>th</sup> August in relation to the time of the day. A total efficiency of about 48% is achieved at around 10 am. A combined maximum efficiency of about 48% is achieved between 10 – 12 am. In case of a non-hybrid system (PV

alone), this corresponds to 6% electrical efficiency as can be deduced from the results obtained. Thus, incorporating a heat collection system has greatly influenced the conversion rate of incoming solar radiation as witnessed from the enhanced efficiency.



**Figure 4.3: The hourly total heat and electrical energy collected versus Total solar radiation**



**Figure 4.4: The hourly efficiency of the Modelled system on 27<sup>th</sup> August, 2014**

## **4.2 Experimental results and discussion**

The experimental results include the overall efficiency of the system, the total amount of energy collected from the system and the water temperatures from the system. The results of August 27, 2014 were randomly chosen to plot graphs to correlate various parameters of the PV/T system

### **4.2.1 Thermal performance**

Figures (4.5) and (4.6) present the panel thermal behaviour when water is flowing through the PV/T collector to effect cooling and when there is no water flowing through the collector respectively. The maximum solar intensity for both cases occurs at around 12 noon. This indicates that the local solar noon for a site within the University of Nairobi is around 12 noon. There is a drastic dip in both solar intensity and average panel temperature at around 1 pm. This is due to cloud cover which lasted for about 30 minutes.

For the case with cooling, the maximum attained panel temperature is  $77.5^{\circ}\text{C}$  whereas for the case with no cooling the maximum is  $83^{\circ}\text{C}$ . Whereas the case with cooling the average panel temperature varies between 39 and  $77.5$ , the temperature for the case with no cooling remains almost constant at a value above  $70^{\circ}\text{C}$  (figure 4.7). The temperature profile of the PV/T corresponds to the intensity as observed in figures (4.5) and (4.6). Figures (4.5) and (4.6) provide vital information on the importance of cooling and give an indication of how much heat energy can be collected from the PV panel by the cooling fluid.

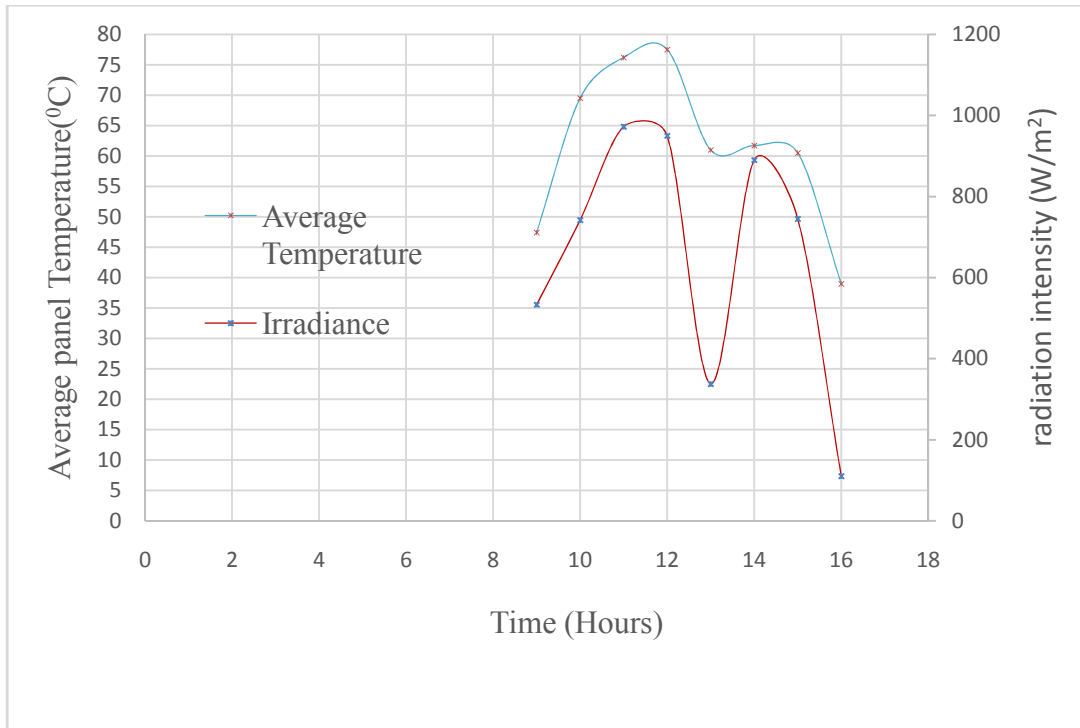


Figure 4.5: Time of day versus radiation intensity and average Panel Temperature for the whole day when water was flowing through the PV/T collector to effect cooling (27<sup>th</sup> August, 2014).

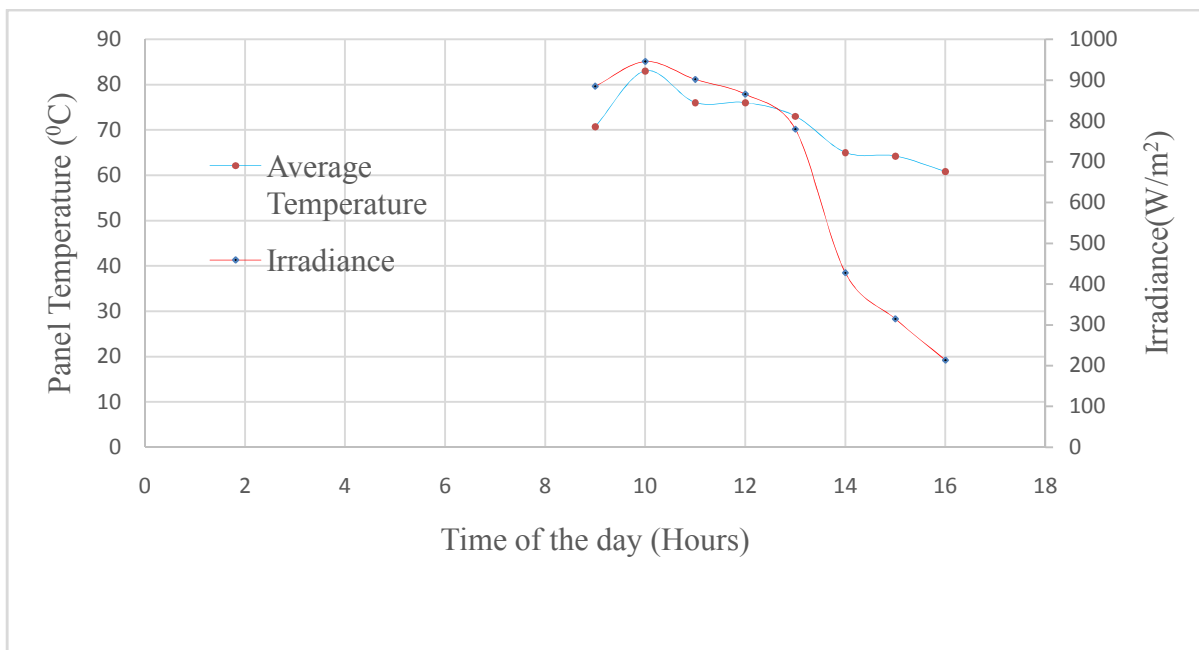
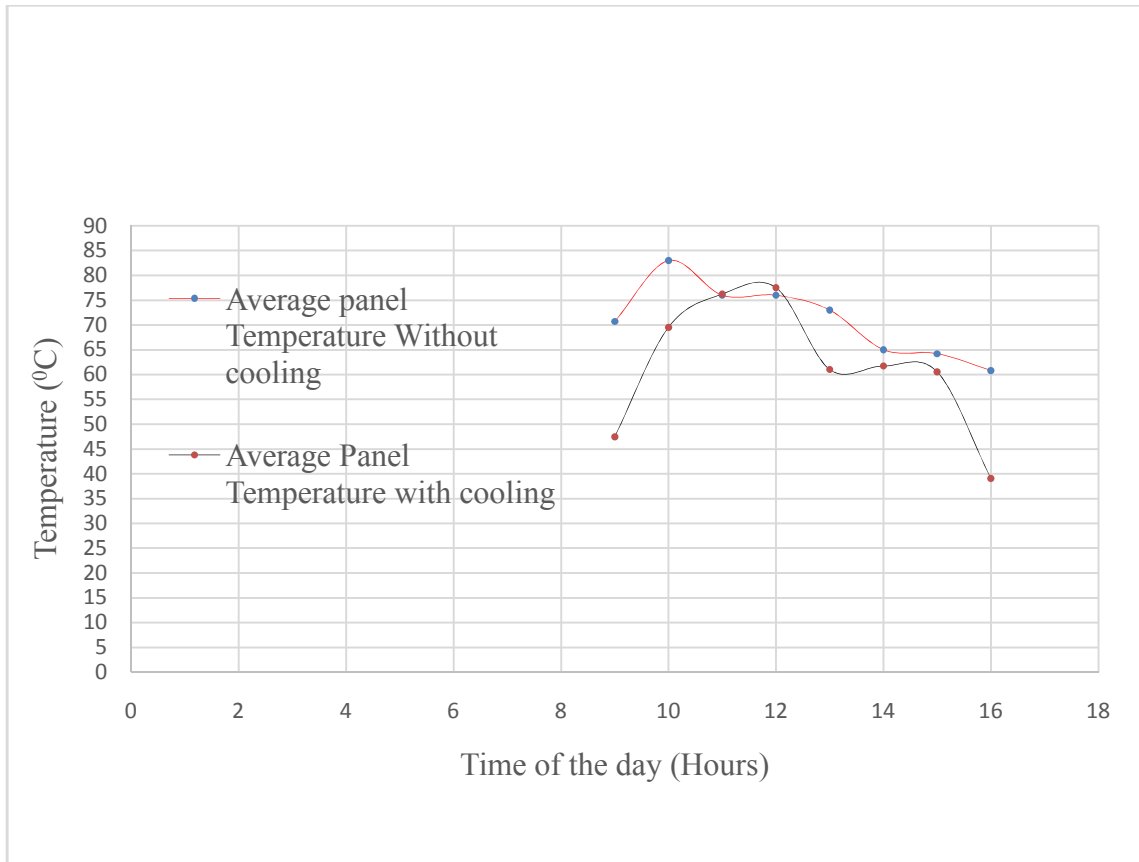
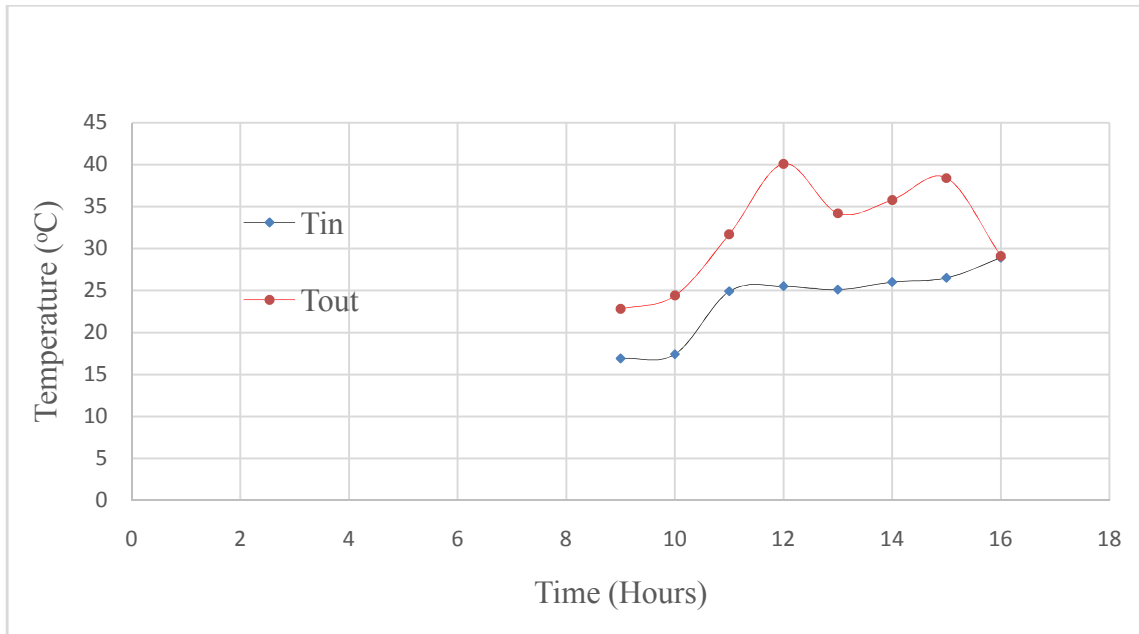


Figure 4.6: Time of day versus radiation intensity and panel Temperature for the whole day when there was no water flowing through the collector (28<sup>th</sup> August, 2014).



**Figure 4.7: Panel temperature profile when water was flowing through the PV/T collector to effect cooling and when water was not flowing (27<sup>th</sup> August, 2014 and 28<sup>th</sup> August, 2014).**

From figure (4.8) it was observed that the maximum temperature difference between inlet and outlet occurs at around 12 noon and it is about 14.6 °C. The minimum temperature difference is about 0.2 °C and occurs at around 4 PM. This temperature difference is attributed to low solar radiation and high ambient temperature. This is because the inlet and outlet water temperatures into and out of the PV/T collector is almost equal.



**Figure 4.8: Temperature profile of inlet and outlet water temperatures from the PV/T panel (27<sup>th</sup> August, 2014)**

From figure (4.9) it can be deduced that the temperature difference between the inlet and outlet will increase by 0.96 °C for every 100 w/m<sup>2</sup> rise in irradiance.

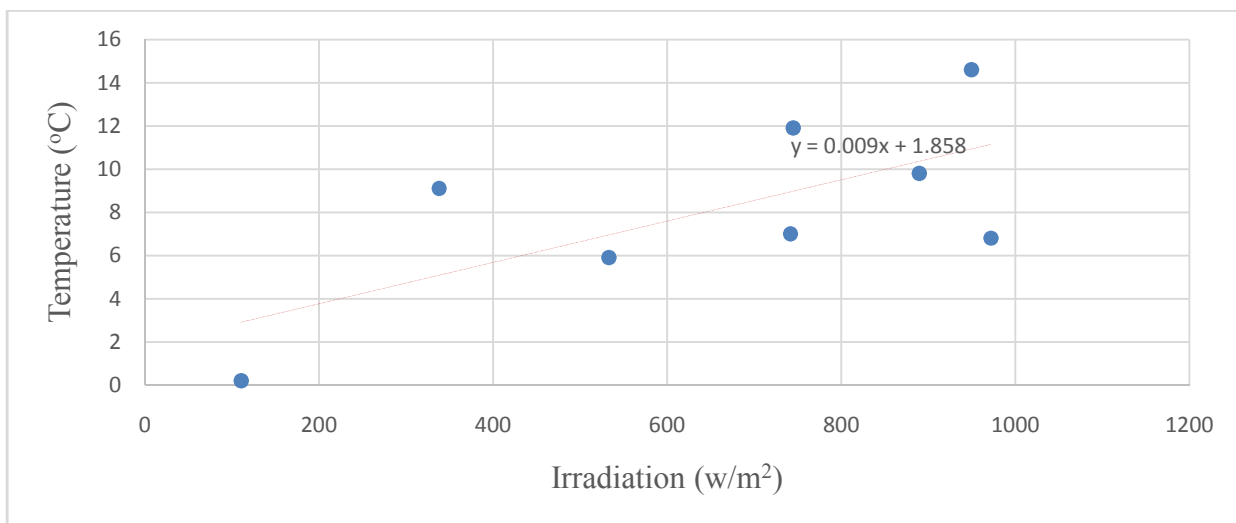


**Figure 4.9: Incident radiation intensity versus variation of water temperature difference between the inlet and outlet channels (27<sup>th</sup> August, 2014)**

Thermal performance of solar energy collectors is always given in terms of efficiency, and it is related to the total incoming radiation. Thermal performance assessment is quite complex since the PV/T collector is part of the thermal system which comprises thermal storage, flow conduits and the supply pump.

The steady state thermal efficiency ( $\eta_t$ ) is given by equation (12) below adopted from Zondag et al. (2005).

$$\eta_t = \frac{\dot{m} c(T_o - T_i)}{GA_c} \quad (12)$$

where G is the measured incoming solar-irradiation on the collector surface ( $W/m^2$ )

The thermal efficiency ( $\eta_t$ ) of PV/T systems is calculated as a function of the ratio shown in equation (13).

$$\frac{\Delta T}{G} \quad (13)$$

where  $\Delta T = T_o - T_i$

It is observed that the thermal efficiencies of the experiment are between 30 and 83% as shown in table (5) and figure (4.10).

**Table 5: Thermal efficiency of the PV/T system (27<sup>th</sup> August, 2014)**

Temperature difference (K)	Irradiance $w/m^2$	Efficiency
278.9	533.0	0.52
280.0	741.7	0.37
279.8	972.2	0.28
287.6	949.7	0.30
282.1	338.0	0.83
282.8	889.8	0.31
284.9	744.8	0.38
273.2	110.5	2.47

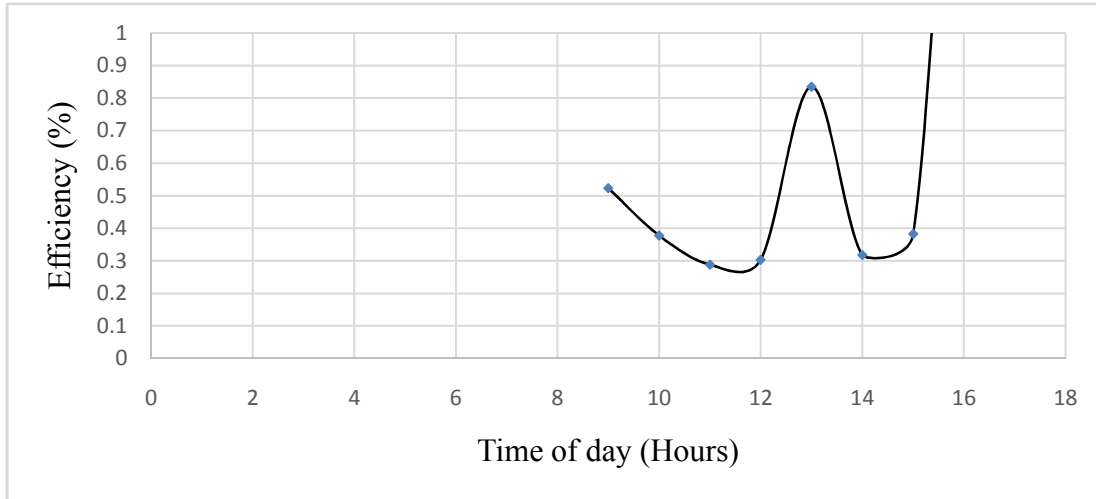


**Figure 4.10: Thermal efficiency against time of the day (27<sup>th</sup> August, 2014).**

The total amount of heat energy collected by the PV/T system on 27<sup>th</sup> August, 2014 is shown in table 6. The total amount of heat energy collected by the water passing through the PV/T collector on 27<sup>th</sup> August, 2014 is 6823.85 kJ. This represents a 46.64 or 47% of the total energy demand for the typical Kenyan family of five.

**Table 6: Total amount of heat energy collected (27<sup>th</sup> August, 2014)**

Time (Hours)	T <sub>in</sub> (°C)	T <sub>out</sub> (°C)	Temperature difference (°C)	Heat Energy collected/ hour (KJ)
9	16.9	22.8	5.9	616.55
10	17.4	24.4	7.0	731.50
11	24.9	31.7	6.8	710.60
12	25.5	40.1	14.6	1525.70
13	25.1	34.2	9.1	950.95
14	26.0	35.8	9.8	1024.10
15	26.5	38.4	11.9	1243.55
16	28.9	29.1	0.2	20.90
<b>Total energy collected/day</b>				<b>6823.85</b>



#### 4.2.2 Electrical Performance

Electrical efficiency ( $\eta_e$ ) is calculated using equation (14) adopted from Zondag et al. (2005)

$$\eta_e = \frac{V_{mpp} I_{mpp}}{GA_c} \quad (14)$$

where  $V_{mpp}$  and  $I_{mpp}$  are the PV module voltage and current respectively at maximum power operation point and  $A_c$  is the effective PV module area.

From figure (4.11) it can be noted that the electrical efficiency range is between 8 and 10%. Temperature differences are a major factor that affects the efficiency of the solar panel. Therefore, it can be concluded that the efficiency values do not fluctuate with very big ranges owing to the stabilized temperature of the panel.

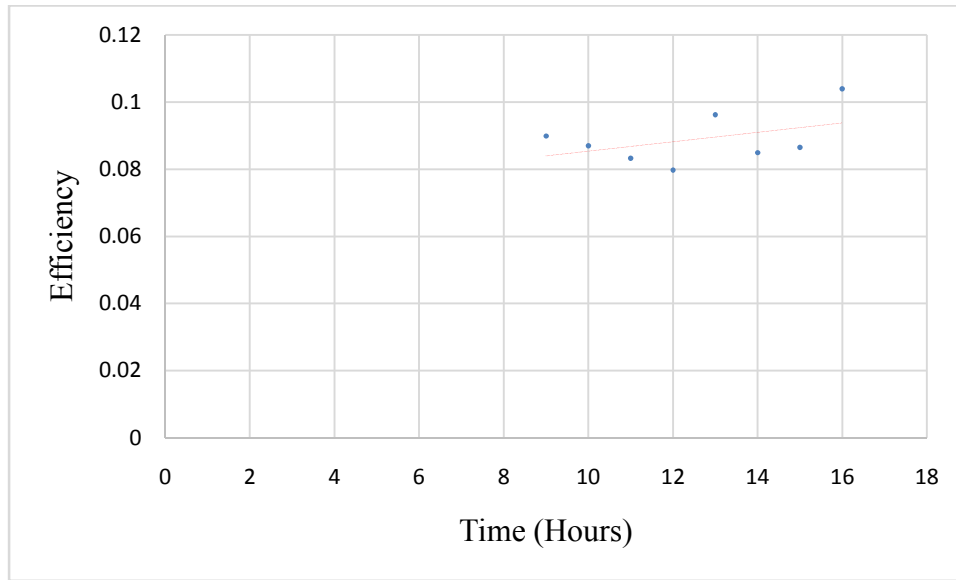


**Figure 4.11: Electrical efficiency against time of the day (27<sup>th</sup> August, 2014).**

The concept of total system efficiency  $\eta_o$  deduced by Wu and Ren (2012) is used to evaluate the overall system performance and is given by equation (15).

$$\eta_o = \eta_t + \eta_e \quad (15)$$

The overall efficiency of the PV/T panel on 27<sup>th</sup> August, 2014 is shown in table 7. It was noted that electrical efficiency of the PV/T panel is relatively stable compared to the thermal efficiency

which fluctuates significantly. This can be attributed to the fact that thermal efficiency is not only a factor of solar radiation but also other factors such as ambient temperature, heat loss to the surroundings, and other meteorological parameters (Chow, 2010). It is observed that the total efficiency of the system is between 37 and 62%. This proves that the overall efficiency of the PV/T system is much higher than that of a separate PV system which ranges up to 10% in practical applications (figure 4.11). This implies that the PV/T system can harness solar energy more adequately as compared to a stand-alone PV system.

**Table 7: Table showing the PV/T panel efficiencies on 27<sup>th</sup> August, 2014**

Time of the day (Hours)	Thermal efficiency of the PV/T panel ( $\eta_t$ )	Electrical efficiency of the PV/T panel ( $\eta_e$ )	Overall Efficiency of the PV/T Panel ( $\eta$ )
0900	0.523	0.090	0.613
1000	0.377	0.089	0.466
1100	0.287	0.083	0.370
1200	0.302	0.080	0.382
1300	0.835	0.096	0.931
1400	0.318	0.085	0.403
1500	0.383	0.086	0.469

### 4.3 Economic Analysis

To determine the economic viability of the PV/T system, the cost of modifying the PV system to hybrid (PV/T) and the extra energy value of the new system were analyzed. A life cycle system cost and savings analysis was performed. In the case of this study, economic analysis is based on discounted payback period analysis.

The discounted payback period is calculated using a return that is greater than 0 %. However, in practice most analysts have used the simple payback period with a no-return requirement (i.e.  $i = 0\%$ ). This is aimed at screening the project to determine if the project requires further consideration. This approach has been criticized since it gives a false picture of an investment's viability. For this reason discounted payback period has been preferred for this kind of analysis

as it incorporates the time value for money. The economic analysis period which is equivalent to the life of the system is taken to be 20 years which was the quoted productive lifespan of the PV module.

The extra energy value is equivalent to the thermal energy output. It is assumed that electricity was used to heat the water. The total amount of heat energy collected on 27 August 2014 (6824 kJ) is equivalent to the electrical energy that was to be used to heat the water. For the whole month of August this would equal to  $(6824 \times 30)$  giving 206698 kJ. Assuming that this electrical energy was to be supplied through the Kenya power and Lighting Company, the saving on electricity for the Kenyan family of five during the month is determined as follows;

206698 KJ is equivalent to 57.42 Kwh or 57.42 units in KPLC terms. The determination of the cost of this amount of power is based on the pre-paid power user guide rev1 (KPLC, 2014).

**Table 8: The cost of buying 57.42Kwh of power from KPLC**

Charge	Rate	Kwh	Concept	Charges (Kshs)
		purchased	Fixed charge	120.00
		57.42	Total Kwh $(57.42 \times 8.1)$	465.10
Fuel	7.83		Fuel Index Charge (Ksh7.83/kwh) i.e. $7.83 \times 57.42$	449.60
Forex	0.94		Forex Charge (Ksh 0.94/kWh) i.e. $0.94 \times 57.42$	53.98
Inflation	0.08		Inflation adjustment (ksh 0.08/Kwh) i.e. $0.08 \times 57.42$	4.59
REP	5%		REP Charge (5%) i.e. $0.05 \times 465.10$	23.26
ERC	0.03		ERC Charge (Ksh 0.03/kWh) i.e. $0.03 \times 57.42$	1.72
VAT	12%		VAT (12%) i.e. $0.12 \times 120$	14.4
Total Cost				1132.65

The monetary saving from the electrical energy per year that results from the system modification is  $(1132.65 \times 12) = \text{Kshs}13591.80$ . The savings from the project was assumed constant per annum.

Table (9) shows the capital investment of modifying the PV module to make it PV/T.

The operation and maintenance costs were assumed negligible given that solar PV and thermal systems require little or no maintenance after commissioning. With the capital investment estimated to be Kshs58, 050 and constant cash saving of Kshs13591.80, the project will repay the invested cash after 5.2 years as shown in table (10) below, which is very satisfactory.

**Table 9: Cost of the additional components required to modify the PV module to PV/T collector.**

Extra components required to modify the PV module	Unit cost (Kshs)	Total cost (Kshs)
6 Pieces Copper tubes (@3.5ft)	875/-	5250/-
150 L solar tank	2300/-	2300/-
Piping and pipe fittings	10,400/-	10,400/-
DC booster pump	27,000	27,000
Insulation box and insulation materials	3100/-	3100/-
Workmanship costs	10,000/-	10,000
<b>Total</b>		<b>58,050/-</b>

**Table 10: Discounted payback period analysis table**

Year	Cash Flow	Present Value factor	Discounted Cash Flow	Cumulative Discounted Cash Flow
0	-58050	1	-58050	-58050
1	13591.8	0.93	12702.61	-45347.38
2	13591.8	0.87	11871.60	-33475.77
3	13591.8	0.81	11094.95	-22380.82
4	13591.8	0.76	10369.11	-12011.70
5	13591.8	0.71	9690.76	-2320.93
6	13591.8	0.66	9056.79	6735.85
7	13591.8	0.62	8464.28	15200.14
8	13591.8	0.58	7910.55	23110.69
9	13591.8	0.54	7393.03	30503.73
10	13591.8	0.50	6909.38	37413.11
11	13591.8	0.47	6457.36	43870.48
12	13591.8	0.44	6034.92	49905.40
13	13591.8	0.41	5640.11	55545.51
14	13591.8	0.38	5271.13	60816.65
15	13591.8	0.36	4926.29	65742.94
16	13591.8	0.33	4604.01	70346.95
17	13591.8	0.31	4302.81	74649.77
18	13591.8	0.29	4021.32	78671.09
19	13591.8	0.27	3758.24	82429.34
20	13591.8	0.25	3512.37	85941.72
Discounted Payback Period	5.15			

## **CHAPTER 5: CONCLUSION AND RECOMMENDATIONS**

### **5.1 Conclusion**

The project investigated a hybrid PV/T system consisting of polycrystalline PV module combined with a water heat extraction unit constructed and tested at the University of Nairobi after modelling and simulation with TRNSYS program. The conclusions from this project can be summarized as below:

1. The optimum water flow rate through the PV/T was determined as 25 L/hour.
2. The combined efficiency of the PV/T system is determined to be 50% on average in practical applications which is way higher than any stand-alone PV system.
3. The lifecycle savings of the system are Kshs 85941 and the payback period is determined as 5.2 years; both figures are quite promising.
4. The system could meet up to 47% of the total heat energy demand for a Kenyan family of five.

### **5.2 Recommendations**

The low value of the optimum flow rate determined from simulation is an indication that the PV/T system could be implemented in thermosyphon mode. This would greatly influence the cost of the overall project since it would eliminate the use of the DC pump which accounts for nearly half of the investment costs. This would further enhance the economic viability of the system since it would reduce the investment costs and the payback period. I recommend that further research should be done excluding a pump and evaluate further the capital saving.

Although a specific application was studied in this project, PV/T systems can be utilized in a variety of applications requiring both electricity and low temperature hot water. The systems would be even more applicable and economic friendly as the cost of solar panels consistently decrease. Thus, I recommend that sustained research should focus on other viable areas of application of PV/T systems.

## References

Boxwell, M. (2012). Solar electricity handbook: A simple, practical guide to solar energy: How to design and install photovoltaic solar electric systems; Greenstream Publishing.

Chow T. T. (2010). A review on photovoltaic/thermal hybrid solar technology. *Applied Energy*. (87)365–379.

Fraunhofer ISE (2016). Photovoltaics Report, updated: 6 June 2016. Accessed at [www.ise.fraunhofer.de](http://www.ise.fraunhofer.de) on 10 August, 2016.

Florschuetz L.W. (1979). Extension of the Hottel-Whillier Model to the Analysis of Combined Photovoltaic/Thermal Flat Plate Collectors. *Solar Energy*. (22), 361-366.

Garg H. P, Agarwal R.K. (1995). Some aspects of a PV/T collector/ forced circulation flat plate solar water heater with solar cells. *Energy Conversion and Management*. (36), 87-99.

Goad C. E. (2012). World climatic zones map. Pearson publishing, Cambridge. 76 – 85.

Government of the republic of Kenya.(2007). Kenya vision 2030.

Hankins M. (2010). Stand-Alone Solar Electric systems: The Earthscan Expert Handbook for Planning, Design and Installation. Earthscan Publishers: London.

Helden, W. van, Zolingen, R.J.Ch. van & Zondag, H.A.(2004). PV Thermal systems: PV panels supplying renewable electricity and heat. *Progress in Photovoltaics: Research and Applications*, 12(6), 415-426.

Hille G. & Franz M. (2011). Grid connection of solar PV: Technical and economic assessment of Net-Metering in Kenya. *Kenya Country Report*.

Hottel, H. C. and Whillier A. (1958). Evaluation of flat-plate solar collector performance. *Transactions of the Conference on Use of Solar Energy*, 2, 74.

Ibrahim A, Othman M.Y, Ruslun M. H, Alghoul M.A, Yahya, Zaharim A & Sopian K. (2009). Performance of Photovoltaic Thermal Collector (PVT) With Different Absorbers Design. *WSEAS transactions on environment and development*, 3(5)321-330.

IEA. (2012). IEA statistics: CO<sub>2</sub> emission from fuel combustion highlights.

IEA. (2011). World Energy Outlook 2011 Factsheet: How will global energy markets evolve to 2035?

Ji J, Chow T. T, He W. (2003). Dynamic performance of hybrid photovoltaic/thermal collector wall in Hong Kong. *Building and Environment*, 38(11), 1327-1334.

Kalogirou S. A & Tripanagnostopoulos Y. (2006). Hybrid PV/T solar systems for domestic hot water and electricity production. *Energy Conversion and Management*, (47) 3368–3382.

Kalogirou S. A. (2009). Solar Energy Engineering: Processes and Systems. Academic press, California.

KPLC (2014). Pre-paid power user guide rev1

Malik A. Q., Ming L. C., Sheng T. K & Blundell M. (2010). Influence of Temperature on the Performance of Photovoltaic Polycrystalline Silicon module in the Bruneian Climate. *AJSTD*, 26(2) 61-72.

NCPD, (2011). Facts and figures on population and development. Available at <http://www.google.co.ke/url?sa=t&rct=j&q=kenya%27s%20population%202011&source=web&cd=6&cad=rja&ved=0CF0QFjAF&url=http%3A%2F%2Fwww.ncpd.ke.org%2Fdocument%2Fd6406cf757208122311cff8dc3170daba8ad3471.pdf>. Accessed on July 16<sup>th</sup> 2016.

Nualboonrueng T, Tuenpusa P, Ueda Y & Akisawa A. (2012). Field Experiments of PV-Thermal Collectors for Residential Application in Bangkok. *Energies*, (5) 1229-1244.

Papadopoulou E. (2011). Photovoltaic industrial systems: An environmental Approach. Springer Science and Business Media.

Tiwari, Arvind, & Sodha M. S. (2006) Performance evaluation of hybrid pv/thermal water/air heating system: A parametric study. *Renewable Energy* 31 (15):2460-2474.

Wei He, Tin-tai Chow, Jie Ji, Jianping Lu, Gang Pei, Lok-shun Chun. (2006). Hybrid photovoltaic and thermal solar-collector designed for natural circulation of water, *Applied Energy*, (83), 199-210.



Wu J. &Ren J. (2012). Research and Application of Solar Energy Photovoltaic-Thermal Technology.*Solar power*.

Zondag H. A, de Vries D. W, Van Helden W. G. J, Van Zolingen R. J. C. & Van Steenhoven A. (2003). The yield of different combined PV-thermal collector designs. *Solar Energy*, (74) 253-269.

Zakharchenko R, Licea-Jimenez L, Perez-GarciaS.A, VorobievP, Dehesa-Carrasco U, Perez-Robles J.F, Gonzalez-HernandezJ, VorobievYu.(2004). Photovoltaic solar panel for a hybrid PV/thermal system.*Solar Energy Materials& Solar Cells*, (82) 253-261.

Zondag H.A, Van der Borg N &Eisenmann W. (2005). PVT performance measurement guidelines: Guidelines for performance measurements of liquid-cooled non-concentrating PVT collectors using c-Si cells. *PV catapult*.

## Appendices

### Appendix A: Experimental Results

#### Appendix A(i): Tables showing results collected from the thermal monitor points

25/08/2014

Time	T <sub>in</sub>	T <sub>out</sub>	T <sub>back</sub>	Curve no.
0830	18.0	19.7	53.4	4
0930	18.4	29.3	59.8	5
1030	25.8	31.3	61.8	7
1130	24.2	34.7	71	8
1230	28.6	29.1	39.6	9
1330	30.8	34.0	76.7	10
1430	25.0	35.0	68.7	11
1530	24.8	33	67	12
1630	24.3	29	56	13

27/08/2014

Time	T <sub>in</sub>	T <sub>out</sub>	T <sub>back</sub>	Curve no.
0900	16.9	22.8	47.4	12
1000	17.4	24.4	69.5	13
1100	24.9	31.7	76.7	14
1200	25.5	40.1	77.5	15
1300	25.1	34.2	61.0	1
1400	26.0	35.8	61.7	2
1500	26.5	38.4	60.5	3
1600	28.9	29.1	39	4

**Appendix A (ii): Table showing Mini-KLA results collected**

PV-curve; curve-no: 12; 8/27/2014 09:00:19 AM

V <sub>mpp</sub> [V]	16.286
I <sub>mpp</sub> [A]	2.940
P <sub>mpp</sub> [W]	47.876
V <sub>oc</sub> [V]	20.456
I <sub>sc</sub> [A]	3.169
G [W/m <sup>2</sup> ]	533.0
T [°C]	42
FF [%]	73.9

PV-curve; curve-no: 13; 8/27/2014 10:00:40 AM

V <sub>mpp</sub> [V]	15.132
I <sub>mpp</sub> [A]	4.260
P <sub>mpp</sub> [W]	64.468
V <sub>oc</sub> [V]	19.867
I <sub>sc</sub> [A]	4.690
G [W/m <sup>2</sup> ]	741.7
T [°C]	53
FF [%]	69.2

PV-curve; curve-no: 14; 8/27/2014 11:00:58 PM

V <sub>mpp</sub> [V]	14.892
I <sub>mpp</sub> [A]	5.432
P <sub>mpp</sub> [W]	80.896
V <sub>oc</sub> [V]	19.956
I <sub>sc</sub> [A]	6.122

**Appendix A (ii) continued**

G [W/m<sup>2</sup>] 972.2

T [°C] 52

FF [%] 66.2

PV-curve; curve-no: 15; 8/27/2014 12:00:24 PM

V<sub>mpp</sub> [V] 13.862

I<sub>mpp</sub> [A] 5.458

P<sub>mpp</sub> [W] 75.665

V<sub>oc</sub> [V] 19.311

I<sub>sc</sub> [A] 6.023

G [W/m<sup>2</sup>] 949.7

T [°C] 59

FF [%] 65.1

PV-curve; curve-no: 1; 8/27/2014 01:00:21 PM

V<sub>mpp</sub> [V] 15.424

I<sub>mpp</sub> [A] 2.107

P<sub>mpp</sub> [W] 32.500

V<sub>oc</sub> [V] 19.652

I<sub>sc</sub> [A] 2.228

G [W/m<sup>2</sup>] 338.0

T [°C] 44

FF [%] 74.2

PV-curve; curve-no: 2; 8/27/2014 02:00:38 PM

V<sub>mpp</sub> [V] 14.680

I<sub>mpp</sub> [A] 5.144

**Appendix A (ii) continued**

Pmpp [W] 75.518  
Voc [V] 19.699  
Isc [A] 5.712  
G [W/m<sup>2</sup>] 889.8  
T [°C] 54  
FF [%] 67.1

PV-curve; curve-no: 3; 8/27/2014 03:00:16 PM

Vmpp [V] 14.709  
Impp [A] 4.376  
Pmpp [W] 64.371  
Voc [V] 19.526  
Isc [A] 4.778  
G [W/m<sup>2</sup>] 744.8  
T [°C] 54  
FF [%] 69.0

PV-curve; curve-no: 4; 8/27/2014 04:00:48 PM

Vmpp [V] 16.592  
Impp [A] 0.692  
Pmpp [W] 11.484  
Voc [V] 19.595  
Isc [A] 0.739  
G [W/m<sup>2</sup>] 110.5  
T [°C] 33  
FF [%] 79.3

Appendix B: Kenya solar resource map (Hill & Franz, 2011)

